Graefes Arch Clin Exp Ophthalmol (2009) 247:421–425
DOI 10.1007/s00417-008-0953-x

CASE REPORT

Nasal and independent polypoidal lesions in polypoidal choroidal vasculopathy

Akiko Okubo · Noriko Abematsu · Taiji Sakamoto

Received: 2 May 2008 / Revised: 5 September 2008 / Accepted: 8 September 2008 / Published online: 11 October 2008

Abstract
Background Polypoidal vessels in polypoidal choroidal vasculopathy (PCV) are known to occur frequently in the macular and peripapillary regions. The aim of this study is to describe patients with polypoidal vessels that are nasal to the optic disc, being independent of macular polypoidal lesions.
Methods A 75-year-old man and a 65-year-old man with polypoidal vessels in the macula of both eyes were followed up through routine examinations including indocyanine green angiography and optical coherence tomography.
Results A polypoidal vessel located 1.5 disc diameters to the nasal margin of the disc was found in the right eye during the first examination in one case, and in the other case it developed during the follow-up period, after successful treatment using photodynamic therapy for the polypoidal lesion in the macula of the left eye. Indocyanine green angiography disclosed no continuity between the polypoidal vessels nasal to the disc and the polypoidal vessels in the macula region in either case. The nasal polypoidal vessels were not associated with exudative changes in either case, and the vessel in one case disappeared spontaneously without any treatment.
Conclusions The findings of this study demonstrate that PCV could involve regions outside the macula and occur in multiple areas independently. The results also indicate the dynamic nature and transitory appearance of polypoidal vessels. Polypoidal vessels nasal to the disc might be overlooked, especially in cases that are not associated with exudative changes, and careful examination might disclose more subclinical nasal polypoidal vessels. Further detailed examination would be helpful to gain a better understanding of the pathogenesis of PCV.

Competing interests The authors have no proprietary interest.

A. Okubo · N. Abematsu · T. Sakamoto
Kagoshima University Graduate School
of Medical and Dental Sciences,
Kagoshima, Japan

A. Okubo (✉)
Department of Ophthalmology, Kagoshima University
Graduate School of Medical and Dental Sciences,
8-35-1 Sakuragaoka,
Kagoshima 890-8520, Japan
e-mail: akiko@m2.kufm.kagoshima-u.ac.jp

Introduction

Polypoidal choroidal vasculopathy (PCV) has typical morphological features: dilated, aneurysmal, polyp-like structures (seen as reddish-orange structures) at the terminations of branching networks of large choroidal vessels, associated with recurrent serosanguineous detachments of the retinal pigment epithelium (RPE) and neurosensory retina and retinal exudation [1, 2]. The vascular abnormality appears to be in the inner choroid, and is composed of two basic elements on indocyanine green angiography (ICG-A): a polypoidal vessel that projects internally from the inner choroid toward the outer retina, and a branching vascular network. Polypoidal vessels have been reported to occur frequently in the macular and peripapillary areas [1, 2], and occasionally in the temporal peripheral fundus [3, 4]. We report on two patients with polypoidal vessels nasal to the optic disc and in the macula independently.

Report of cases

Case 1

A 75-year-old Japanese man presented with a 1-year history of decreased visual acuity in the left eye; the best corrected

visual acuity was 20/25 OD and 20/2000 OS. Examination of the left eye revealed several reddish-orange nodules suggesting polypoidal vessels, with serous retinal detachment and hard exudates in the macula. In the asymptomatic right eye, a focal elevated yellow lesion and a reddish-orange lesion (Fig. 1a, *arrows*) were observed inferior and superior to the centre of the fovea respectively. No associated exudative changes were seen, and the centre of the fovea revealed slight atrophic changes of the RPE. ICG-A, which was obtained using a fundus camera (TRC-50LX/IMAGnet, Topcon, Tokyo, Japan), revealed vascular networks that terminate in polypoidal vessels in the left eye, and polypoidal vessels inferior and superior to the centre of the fovea (Fig. 1b, *arrows*) in the right eye. PCV was diagnosed in both eyes. Funduscopic examination of the nasal quadrant in the right eye revealed a yellow nodule (Fig. 1a, *arrowhead*), which was shown as a focal elevation of the RPE by optical coherence tomography (Fig. 1a, *inset*), with slight atrophy of the RPE peripherally, 1.5 disc diameters to the nasal margin of the disc. The nodule was confirmed as a polypoidal vessel with ICG-A (Fig. 1b, *arrowhead*), having no continuity with the polypoidal vessels in the macula. The colour images and ICG-A were acquired by moving the camera head to the nasal side using a 50-degree lens. The patient was treated with two sessions of photodynamic therapy (PDT) using verteporfin (Visudyne, Novartis) in the left eye. The right eye was followed without any treatment, because the polypoidal lesion in the macula had not shown any significant changes and maintained good visual acuity (20/25) during the follow-up period of 31 months. Five months after the initial presentation, the nasal polypoidal vessel had disappeared when assessed by ICG-A (Fig. 1c), which was performed during a regularly scheduled follow-up visit to evaluate the necessity of retreating the left eye.

Case 2

A 65-year-old Japanese man, having decreased vision, with a prior history of laser photocoagulation for fundus hemorrhage 15 years before in the right eye was referred for evaluation. Best corrected visual acuity was 20/25 OD

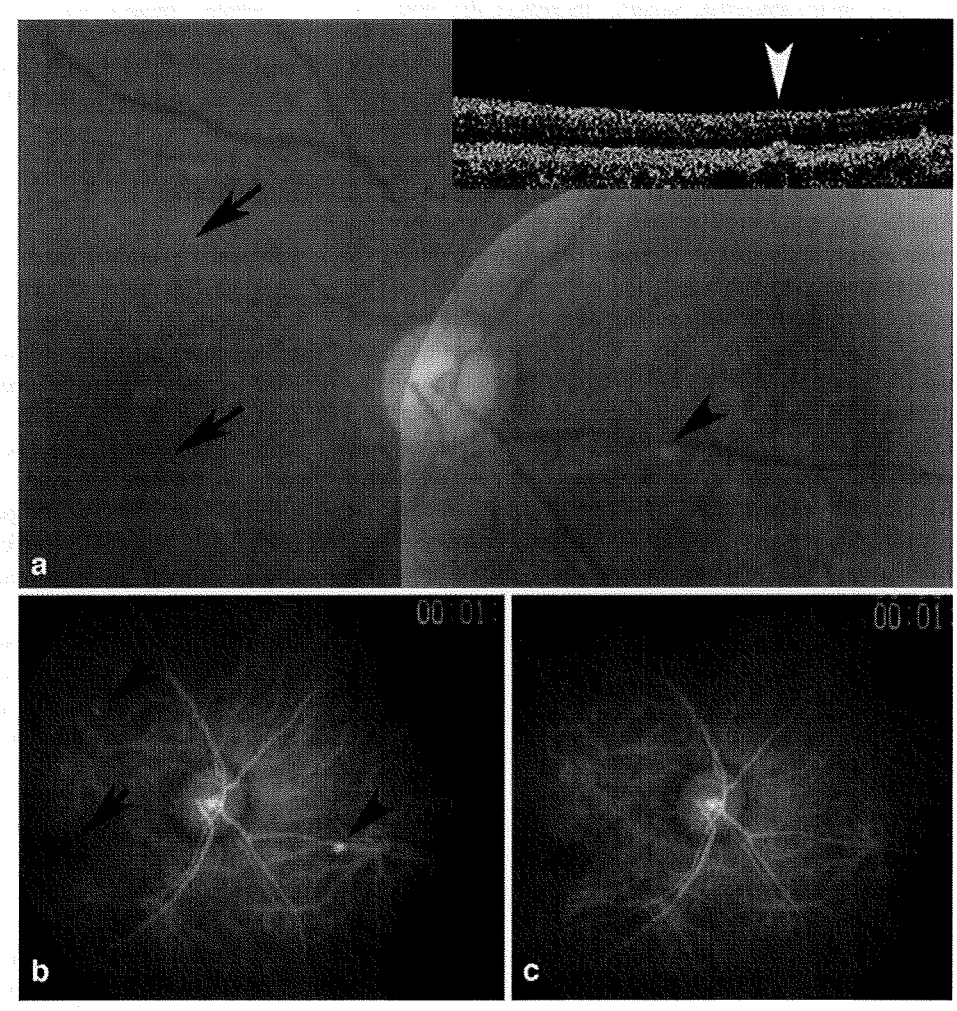

Fig. 1 **a** Fundus photograph of the right eye of case 1 at presentation showing focal elevated lesions (*arrows*) inferior and superior to the centre of the fovea, without exudative changes, and a yellow nodule (*arrowhead*) 1.5 disc diameters to the nasal margin of the disc, with slight atrophic change of the retinal pigment epithelium (RPE). *Inset*: optical coherence tomography (OCT) performed over the nasal lesion horizontally shows focal elevation of the RPE (*white arrowhead*). **b** Early phase of the indocyanine green angiography (ICG-A) at presentation reveals three polypoidal vessels (*arrows and arrowhead*) corresponding to the elevated lesions. The continuity between the polypoidal vessels in the macula and the polypoidal vessel nasal to the disc was not seen. **c** Early phase of the ICG-A taken 5 months after presentation showing the disappearance of the nasal polypoidal vessel

and 20/16 OS. Ophthalmoscopic examination of the right eye revealed a few reddish-orange nodules with hard exudates and serous retinal detachment in the macula; ICG-A revealed a few polypoidal vessels corresponding to the reddish-orange nodules. Ophthalmoscopic examination of the asymptomatic left eye revealed a few reddish-orange nodules inferior to the centre of the fovea, without any exudative changes such as detachment of the RPE and neurosensory retina, and hard exudates (Fig. 2a). ICG-A of the left eye showed polypoidal vessels corresponding to the reddish-orange nodules in the macula and choroidal hypofluorescence, within which a few dilated choroidal vessels were seen superior to the disc (Fig. 2b, *arrow*). The latter lesion showed slight atrophy of the RPE without elevation. At the first examination, no polypoidal lesions were observed in the nasal quadrants in either eyes. He was diagnosed as having PCV in both eyes. The right eye was treated with two sessions of PDT. Due to serous retinal

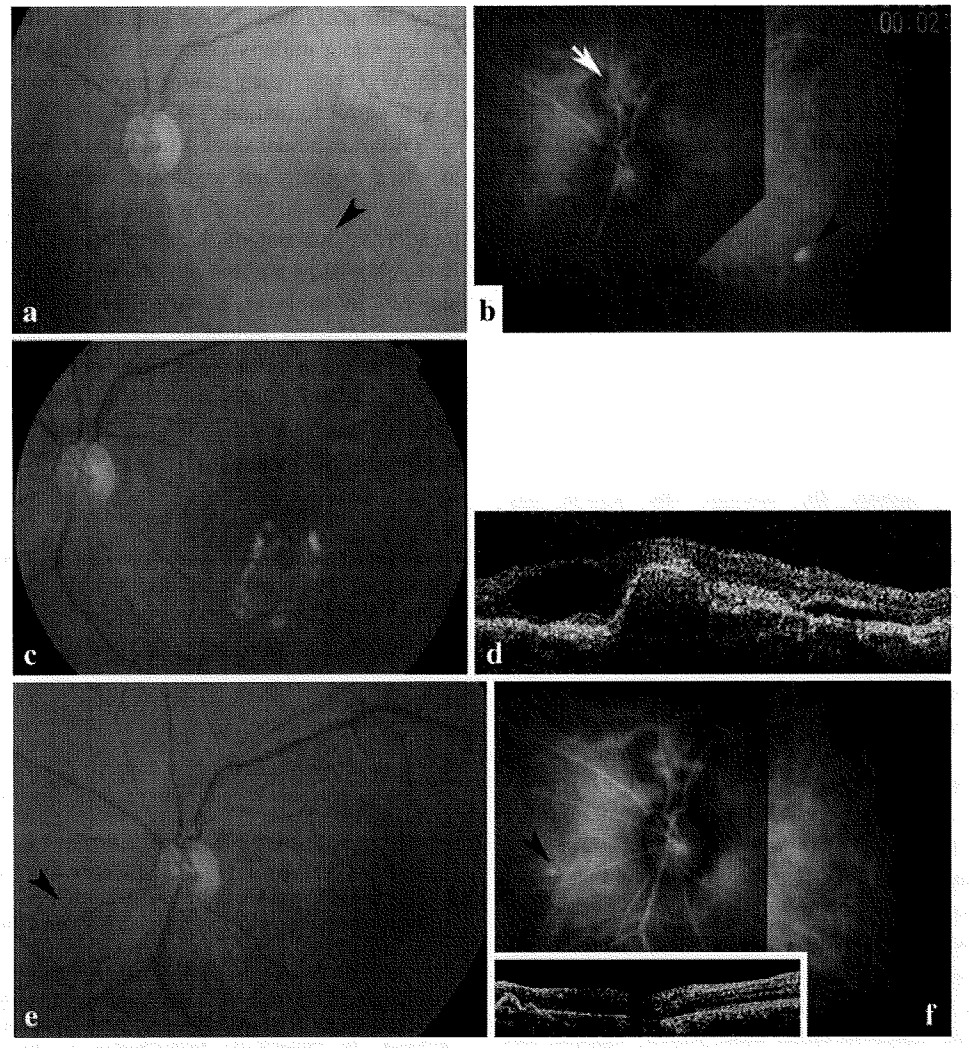

Fig. 2 **a** Fundus photograph of the left eye of case 2 at presentation, showing a few reddish-orange nodules inferior to the centre of the fovea (*arrowhead*) without exudative changes. **b** ICG-A at presentation reveals polypoidal vessels (*arrowhead*) corresponding to the reddish-orange nodules in the macula and area of choroidal hypofluorescence, within which a few dilated choroidal vessels (*arrow*) were seen superior to the disc. **c** Fundus photograph at 30 months after presentation and before the first photodynamic therapy (PDT), showing serous detachment of neurosensory retina, with hard exudates in addition to the reddish-orange nodules in the macula. **d** OCT performed over the macular lesion at 30 months after presentation reveals focal elevation of the RPE with serous retinal detachment and cystic macular edema. **e** Fundus photograph at 3 months after the second PDT showing disappearance of the reddish-orange lesion, serous retinal detachment and hard exudates. Of note is a new solitary small reddish-orange nodule (*arrowhead*) occurring 1.5 disc diameters from the nasal disc margin. **f** ICG-A taken 3 months after the second PDT, showing disappearance of polypoidal vessels in the macula and appearance of a polypoidal vessel (*arrowhead*) corresponding to the new reddish-orange nodule. The continuity between the nasal polypoidal vessel and the original polypoidal lesion in the macula was not shown. *Inset*: OCT performed over the nasal polypoidal vessel horizontally showing focal elevation of the RPE

detachment and hard exudates that developed in the left eye, and a decreased visual acuity of 20/40 (Fig. 2c,d), the left eye was also treated with PDT to cover the polypoidal vessels in the macula 30 and 34 months after initial presentation. According to the standard protocol, fluorescein green angiograms were evaluated to determine the greatest linear dimension (GLD), and a 689-nm diode laser was applied for 83 seconds with a light dose of 50 J/cm^2. The GLD at each time was 4100μm and 3700μm respectively. Three months after the second PDT, the polypoidal vessels in the macula and serous retinal detachment disappeared, but a new solitary small polypoidal vessel occurred 1.5 disc diameters from the nasal optic disc margin (Fig. 2e,f). The continuity between the nasal polypoidal vessel and the original polypoidal lesion in the macula was not shown. The nasal polypoidal vessel was not associated with serous/hemorrhagic detachment of the RPE and neurosensory retina, nor hard exudates until the last follow-up examination (23 months after the appearance of the nasal polypoidal vessel). Visual acuity remained stable at 20/32.

Discussion

The findings of this study demonstrate that PCV could involve regions outside the macula. The results also indicate the dynamic nature and transitory appearance of polypoidal vessles.

The patients presented here had typical polypoidal lesions in the macula of both eyes. Polypoidal vessels were also observed 1.5 disc diameters to the nasal margin of the disc. The nasal polypoidal vessel was found during the first examination of case 1, while in case 2 it developed during the follow-up period after successful treatment of the polypoidal vessels in the macula. The nasal polypoidal vessel in case 1 disappeared without any treatment, and the vessels in both cases were not associated with any exudative changes. It is difficult to conclude that nasal polypoidal vessels are less active than polypoidal vessels in the macula, because some polypoidal vessels in the macula were also reported to disappear spontaneously.

Notably, the nasal polypoidal vessel showed no continuity with the macular lesion in either case, which suggests that polypoidal vessels could occur in multiple areas independently. Regarding the location of pathologic vessels, choroidal neovascularization in typical exudative age-related macular degeneration (AMD) is known to occur in the macula mainly, while polypoidal vessel formation in PCV occurs frequently in the macular and the peripapillary regions. Recently, genetic differences in the elastin gene between patients with neovascular AMD and patients with PCV have been reported [5], supporting previously reported different histopathologic aspects of the two diseases in Bruch's membrane and in the walls of pathologic vessels containing elastic layers. In clinicopathologic studies of patients with PCV, altered RPE–Bruch's membrane–choriocapillaris complex and underlying arterioles with marked sclerotic changes and dilated venules were observed [6–8]. In addition, cavernous vascular channels that originated from branches of the short posterior ciliary arteries (PCAs) were documented in another clinicopathologic report [9]. Indeed, the location of frequently occurring polypoidal vessels in the macular and peripapillary areas, and even the nasal area to the disc, would overlap the entry sites of short PCAs [10]. The RPE–Bruch's membrane–choriocapillaris complex in those areas where such relatively large vessels enter may be susceptible to polypoidal vessel formation.

Nasal polypoidal vessels might be overlooked, especially in cases that are not associated with exudative changes, such as the two cases presented. In addition, this nasal location is just out of the field when colour images and ICG-A are taken without moving the camera head or asking patients to look in a particular direction consciously. Ophthalmologists should be aware that polypoidal vessels can occur not only in the macular and peripapillary region but also in the nasal region to the disc. Further detailed examinations would be helpful to gain a greater understanding of the pathogenesis of PCV.

Grant information This work was supported by research grant number 19592028 from the Japanese Ministry of Education, Science, Sports, and Culture.

References

1. Ciardella AP, Donsoff IM, Huang SJ, Costa DL, Yannuzzi LA (2004) Popypoidal choroidal vasculopathy. Surv Ophthalmol 49:25–37
2. Sho K, Takahashi H, Wada M, Nagai Y, Otsuji, Nishikawa M, Mitsuma Y, Yamazaki Y, Matsumura M, Uyama M (2003) Polypoidal choroidal vasculopathy: incidence, demographic features, and clinical characteristics. Arch Ophthalmol 121:1392–1396
3. Yannuzzi LA, Nogueira FB, Spaide RF, Guyer DR, Orlock DA, Colombero D, Freund KB (1998) Idiopathic polypoidal choroidal vasculopathy: a peripheral lesion. Arch Ophthalmol 116:382–383
4. Merle H, Donnio A, Jean-Charles A (2007) Vasculopathie polypoidale choroidienne idiopathique peripherique. Can J Ophthalmol 42:631–632
5. Kondo N, Honda S, Ishibashi K, Tsukahara Y, Negi A (2008) Elastin gene polymorphisms in neovascular age-related macular degeneration and polypoidal choroidal vasculopathy. Invest Ophthalmol Vis Sci 49:1101–1105
6. Okubo A, Sameshima M, Uemura A, Kanda S, Ohba N (2002) Clinicopathological correlation of polypoidal choroidal vasculopathy revealed by ultrastructural study. Br J Ophthalmol 86:1093–1098
7. Kuroiwa S, Tateiwa H, Hisatomi T, Ishibashi T, Yoshimura N (2004) Pathologic features of surgically excised polypoidal

choroidal vasculopathy membranes. Clin Exp Ophthalmol 32:292–302
8. Nakajima M, Yuzawa M, Shimada H, Mori R (2004) Correlation between indocyanine green angiographic findings and histopathology of polypoidal choroidal vasculopathy. Jpn J Ophthalmol 48:249–244
9. Rosa RH Jr, Davis JL, Eifrig CW (2002) Clinicopathologic correlation of idiopathic polypoidal choroidal vasculopathy. Arch Ophthalmol 120:502–508
10. Hayreh SS (2004) Posterior ciliary artery circulation in health and disease. The Weisenfeld lecture. Invest Ophthalmol Vis Sci 45:749–757

Ultrasound in Med. & Biol., Vol. ■, No. ■, pp. 1–9, 2009

0301-5629/09/$–see front matter

ELSEVIER

doi:10.1016/j.ultrasmedbio.2009.05.023

● *Original Contribution*

SONOTHROMBOLYSIS FOR INTRAOCULAR FIBRIN FORMATION IN AN ANIMAL MODEL

TOSHIFUMI YAMASHITA,* HIROKI OHTSUKA,* NOBORU ARIMURA,* SHOZO SONODA,* CHIHIRO KATO,† KANEO USHIMARU,† NAOKO HARA,† KATSURO TACHIBANA,‡ and TAIJI SAKAMOTO*

*Department of Ophthalmology, Kagoshima University Graduate School of Medical and Dental Sciences, Sakuragaoka, Kagoshima, Japan; †Tomey Corporation, Nagoya, Aichi, Japan; and ‡Department of Anatomy, Faculty of Medicine, Fukuoka University, Fukuoka, Japan

(*Received* 17 *October* 2008, *revised* 22 *May* 2009, *in final form* 28 *May* 2009)

Abstract—Vascular diseases such as diabetic retinopathy or retinal arterial occlusion are always associated with retinal and/or choroidal vasculopathy and intravascular thrombosis is commonly found. The ultrasound (US) therapy is a recently developed technique to accelerate fibrinolysis and it is being applied to some clinical fields. The present study was to observe the effects of extraocular US exposure on intraocular fibrin, which is a deteriorating factor in various ocular diseases. Tubes containing human blood (2 mL) in the following groups were irradiated with US; US alone, US with tissue plasminogen activator (tPA), tPA alone, and saline (control). Fibrinolysis was quantified by measuring D-dimer after 2 h. In rat eyes, intracameral fibrin (fibrin formation in the anterior chamber of the eye) was induced by YAG-laser-induced iris bleeding. Then, eyes in the following groups were irradiated with US; US alone, subconjunctival tPA alone, US and subconjunctival tPA, control. Intracameral fibrin was scored on day 3 (3+ maximum to 0). The temperatures of rat eyes were measured by infrared thermography. Histologic evaluation was also performed. D-dimer was increased by US with statistical significance ($p < 0.05$) or tPA ($p < 0.01$). D-dimer in US with tPA group was significantly higher than either US alone or tPA alone group ($p < 0.01$). In rat eyes, the average intracameral fibrin score on day 3 was 1.4 in control group and 1.2 in subconjunctival tPA alone group; however, it decreased significantly in the US alone group (0.75; $p < 0.05$, vs. control), US and subconjunctival tPA group (0.71; $p < 0.01$, vs. control). The temperature was less than 34 °C after US exposure. No histologic damage was observed. US irradiation from outside accelerated intracameral fibrinolysis without causing apparent tissue damage. This noninvasive method might have therapeutic value for intraocular fibrin. (E-mail: tsakamot@m3.kufm.kagoshima-u.ac.jp) **© 2009 World Federation for Ultrasound in Medicine & Biology.**

Key Words: **Ultrasound, Fibrinolysis, Thrombolysis, Sonothrombolysis, Tissue plasminogen activator.**

INTRODUCTION

Vascular diseases such as diabetic retinopathy are the leading causes of legal blindness in adults in western societies. These diseases are always associated with retinal and/or choroidal vasculopathy and intravascular thrombosis is commonly found to some extent (Vine and Samama 1993). Among them, retinal arterial occlusion (RAO) has a poor prognosis (Hayreh 2008). Furthermore, fibrin formation in the vitreous and/or anterior chamber is sometimes observed after intraocular surgery, leading to secondary tissue damage (Akassoglou et al. 2004; Jaffe et al. 1990; McDonald et al. 1990; Toth et al. 1991). To remove thrombus or fibrin, a fibrinolytic agent such as tissue-plasminogen activator (tPA) is sometimes used (Feltgen et al. 2006; Hayreh 2008; Kattah et al. 2002; Noble et al. 2008; Richard et al. 1999; Weber et al. 1998). However, the effect of fibrinolytic agents on these diseases is controversial and the potential toxicity of high doses of tPA cannot be neglected (Yamamoto et al. 2008; Yoeruek et al. 2008). Surgical removal of intravascular thrombus is another approach but its therapeutic value is also controversial (García-Arumí et al. 2006; Opremcak et al. 2008). Above all, the invasiveness and the potential risks of surgical embolus removal would make it difficult for physicians to accept these treatments.

The use of ultrasound (US) to accelerate fibrinolysis for thrombolytic therapy is a developed technique. It was

Address correspondence to: Taiji Sakamoto, Department of Ophthalmology, Kagoshima University Graduate School of Medical and Dental Sciences, Sakuragaoka, Kagoshima, Kagoshima 890-8520, Japan. E-mail: tsakamot@m3.kufm.kagoshima-u.ac.jp

evaluated by previous studies and has been found to have effects but less invasive potential for fibrinolysis (Francis et al. 1992; Holland et al. 2008; Hong et al. 1990; Lauer et al. 1992; Tachibana 1992; Tachibana K and Tachibana S 1995, 1997; Trübestein et al. 1976). Therefore, it is being applied in some clinical fields including peripheral vascular occlusions, acute myocardial infarctions (Cohen et al. 2003), occluded arteriovenous dialysis grafts (Pfaffenberger et al. 2005) and acute ischemic stroke. Early investigators showed that transcranial US increases fibrinolytic activity (Francis et al. 1995). Although a translational study using large US probes was hampered by an increased rate of intracerebral hemorrhage, phase-II Combined Lysis of Thrombus in Brain Ischemia Using Transcranial Ultrasound and Systemic t-PA trial that randomly assigned 126 patients with middle cerebral artery occlusion showed favorable results (Alexandrov et al. 2004; Daffertshofer et al. 2005).

In comparison to intracranial or visceral lesions, intraocular lesion is expected to be suitable for this treatment because responses to the treatment can be monitored in detail by direct observation and the therapeutic efficacy might be achievable with less power. So far, to the best of our knowledge, there have been no reports on sonothrombolytic treatment for ocular fibrin formation. In this study, we report on this new promising treatment approach for intracameral fibrin (fibrin formation in the anterior chamber of the eye) and evaluate its effects.

MATERIALS AND METHODS

In vitro study

Fibrin clot preparation. Venous blood was withdrawn from four healthy volunteers after they provided informed consent. Whole blood (2 mL) was immediately placed in disposable culture tubes. The tubes containing the blood were then placed in a 37°C water bath for 2 h referring to the previously described method (Frenkel et al. 2006).

US treatment. US was irradiated using a commercially available machine (Sonitron 2000; Richmar, Inola, OK, USA) with a 6 mm unfocused probe directly to the blood in the tubes (Borex, 12 × 75 mm disposable culture tubes, composed of borosilicate glass) in a tank of water at 37°C for various time intervals. Based upon our preliminary experiment, the parameters of US were determined as follows: frequency of 1.0 MHz, duty cycle of 5.2%, pulse repetition frequency of 20 Hz and the derated spatial-peak pulse-average intensity ($I_{SPPA.3}$) of 10.123 W/cm^2. First, US was irradiated with different exposure times, 5 min or 20 min (n=8, each). In addition, the temperature in the tube was measured after US irradiation for 20 min under the same condition (n = 4). Next, the experimental groups were divided into the following: US exposure alone (US, n = 8), US exposure with tPA (US + tPA, n = 8), tPA alone (tPA, n = 8) and saline alone (no US, no tPA, control, n = 8). tPA (Cleactor; Eisai, Tokyo, Japan) was diluted with saline (40 IU/μL) just before the experiment. Before the clots were exposed to US, tPA and saline (total 500 μL) were added to the tubes and incubated in a 37°C water bath for 2 h.

D-dimer assays. Because D-dimer is an indicator of fibrin-degraded products, a commercial D-dimer assay kit (Diagnostica Stago, Parsippany, NJ, USA) was used to measure D-dimer levels 2 h after treatment. The assays were performed according to directions provided by the manufacturer.

In vivo study

Safety of US exposure. Before application of US with animals, the output level of US was evaluated. We examined the safety of Sonitron 2000 with a 3 and 6 mm unfocused probes in consideration of application to human eyes. In brief, we measured acoustic power using a needle hydrophone in a water tank and assessed and computed some acoustic parameters (Schema 1). US was irradiated under the following conditions: frequency of 1.0 MHz, high or low intensity mode indicated on the device and duty cycle of 5.2% or 100%. Safety conditions referred to information of manufacturers seeking marketing clearance for diagnostic ultrasound systems and transducers by the Food and Drug Administration of the United States Department of Health and Human Services (FDA) (http://www.fda.gov/cdrh/ode/guidance/560.html#2).

Animals. All animals were used humanely in accordance with the approval of our institutional animal care committee and the ARVO statement on the Use of Animals in Ophthalmic and Vision Research. Brown-Norway rats (male; age 8-weeks old, 250 g) were purchased from KBT Oriental Co., Ltd. (Fukuoka, Japan).

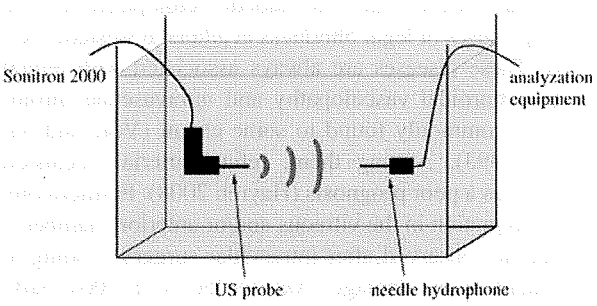

Schema 1. The simplified schema of the measurement system to evaluate the output level of US. Measurement system using a needle hydrophone in a water tank to assess and compute some acoustic parameters of Sonitron 2000 with a 3 and 6 mm unfocused probes.

Induction of intracameral fibrin clot formation and evaluation. In each of the following procedures, Brown-Norway rats were anesthetized with an intramuscular injection of ketamine hydrochloride (50 mg/kg) and xylazine hydrochloride (20 mg/kg), and the ocular surface was anesthetized with a topical instillation of 0.2% oxybuprocaine hydrochloride eye drops (Santen Pharmaceutical Co., Ltd., Osaka, Japan). Intracameral bleeding was induced by a neodymium-doped yttrium aluminium garnet (Nd:YAG) laser according to previous report (Sakamoto et al. 1999). Nd:YAG laser radiation on the iris is a standard treatment in clinical ophthalmology for glaucoma and appears to be a safe (Drake 1987; Tomey et al. 1987). In this study, laser radiation was performed by the Q-switched Nd:YAG laser system mounted on a slit lamp (Ellex Japan Inc., Osaka, Japan) using energy setting of 1.2 mJ per shot and single pulse mode. Nd:YAG laser were shot at six points on the iris (0, 2, 4, 6, 8 and 10 o'clock) with the spot size of 8 μm. In order to confirm the selectivity of YAG laser treatment, three eyes were enucleated immediately and fixed with 3.7% formaldehyde in phosphate buffered saline (PBS), dehydrated with a graded alcohol series and embedded in paraffin. The sections were cut and stained with hematoxylin and eosin. All of the specimens were then observed by two masked observers who received no information about the specimens. After laser shots, moderate to severe bleeding occurred immediately, clot and fibrin was discerned on the surface of the iris and lens on the next day. The value of clot formation in the anterior chamber was graded using surgical microscopy according to the previously described method (Sakamoto et al. 1999). Briefly, the criteria were defined as follows: 3+, clot or bleeding occupies more than one-third of the anterior chamber; 2+, between one-fifth and one-third of anterior chamber; 1+, less than one-fifth of anterior chamber; 0, no clot or bleeding. The eyes were observed by surgical microscopy everyday and photographs were taken on the next day (day 1) and fourth day (day 3) by masked observers.

Sonothrombolysis. The day after the laser shots, a 3 mm US probe was placed directly onto the corneal surface, coupling with a gel, hydroxyethyl cellulose (Senju Pharmaceutical Co. Ltd., Osaka, Japan) of the rats under general anesthesia and US was irradiated. The parameters of US were set at frequency of 1.0 MHz, duty cycle of 5.2%, pulse repetition frequency of 20 Hz and $I_{SPPA.3}$ of 0.228 W/cm^2 and US was irradiated for 5 min and the experimental groups were divided as follows: US alone (US group, $n = 14$), US and subconjunctival tPA (US and subconjunctival tPA group, $n = 14$), subconjunctival tPA alone (tPA group, $n = 14$) and no treatment (control, $n = 14$). When t-PA was applied, 50 μL of t-PA (2000 IU) after diluting with saline (final concentration 40 IU/μL) was injected into the center of the tarsal conjunctiva using a syringe with a 30-gauge needle under surgical microscopy. Given that tPA weights 68 kDa, subconjunctival injection of tPA would have a limited effect, however, the thrombus was dissolved even a little intracameral administration in our preliminary study. So, this method was done as a topical administration.

Ocular surface temperature and histologic findings. Brown-Norway rats were first anesthetized as described above. A 3 mm US probe was placed directly onto the corneal surface and US was irradiated under the following conditions: frequency of 1.0 MHz, high intensity mode (indicated on the device) and duty cycle of 5.2% or 100%. The temperature was monitored for 5 min using infrared thermography (TH6200R, NEC Co., Ltd., Tokyo, Japan). For the microscopic analysis, the eyes were enucleated after 48 h and were examined histologically the same way as above. More than six eyes of each group were examined.

Statistical analysis. All values were expressed as mean ± SD. Analysis of variance with paired *t*-test was used to determine the significance of the difference in a multiple comparison. Differences with a p value of less than 0.05 were considered to be significant.

RESULTS

In vitro study

US exposure time. US exposure was examined under the above conditions for 5 min or 20 min (exposure time). The results showed that D-dimer was significantly increased by US exposure and that 20 min exposure of US resulted in significantly higher levels than 5 min exposure (Fig. 1, $p < 0.01$). In this condition, there was no

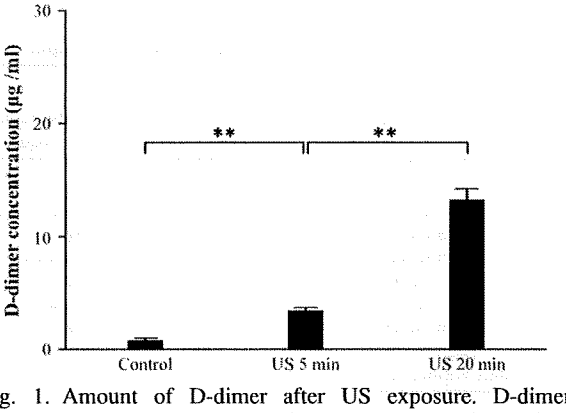

Fig. 1. Amount of D-dimer after US exposure. D-dimer increased after US exposure in a time-dependent fashion (paired *t*-test, $^{**}p < 0.01$). Control; neither US nor tPA.

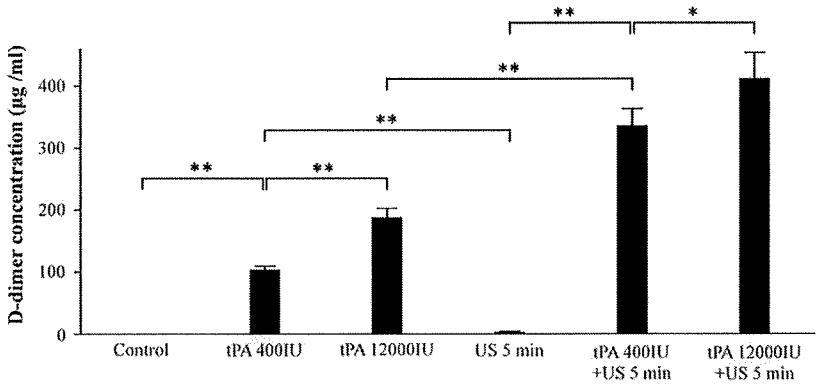

Fig. 2. Amount of D-dimer after US exposure and tPA. D-dimer was increased by tPA in a dose dependent fashion. Simultaneous US exposure and tPA significantly increased the amount D-dimer (paired t-test, $*p < 0.05$, $**p < 0.01$).

change in temperature from 37°C after US exposure in all experiments.

Effects of US and tPA. D-dimer was significantly increased by tPA application and also showed a dose-dependent effect (Fig. 2, $p < 0.01$). Because 5 min exposure was sufficient to obtain treatment effects, the following US exposure times were fixed for 5 min. As a result, D-dimer was increased by tPA in a dose-dependent fashion. Simultaneous US exposure and tPA significantly increased D-dimer (Fig. 2).

Safety of US exposure. With a 6 mm probe, $I_{SPPA.3}$ was less than 28 W/cm^2 but the derated spatial-peak temporal-average intensity ($I_{SPTA.3}$) was far more than 17 mW/cm^2 in all conditions. With a 3 mm probe, $I_{SPPA.3}$ was less than 28 W/cm^2 and $I_{SPTA.3}$ was also less than 17 mW/cm^2 under the condition of a duty cycle of 5.2%. All computed acoustic parameters were referred in Table 1.

In vivo study

Sonothrombolysis. Before US irradiation, the fibrin score was approximately 2.4 and there were no statistical differences between groups. In the controls, intracameral fibrin clot decreased gradually over time, and the average score on day 3 was 1.4 ± 0.21. While eyes that received subconjunctival tPA injection alone showed a slight decrease of clots, and the average score was 1.2 ± 0.19. There was no statistically significant difference with controls. In contrast, eyes that received US alone or both subconjunctival tPA and US showed apparent decreases of clots and the average scores decreased to 0.75 ± 0.13 and 0.71 ± 0.11, respectively (control vs. US alone; $p < 0.05$ and control vs. US with subconjunctival tPA; $p < 0.01$) (Figs. 3 and 4). During the experimental course, no pathologic change such as edema or new bleeding was observed in any of cornea, anterior chamber, iris or lens by surgical microscopic observation (Fig. 4).

Ocular surface temperature. Before US exposure, the surface temperature was approximately 25°C (less than 32 °C in the periocular area) (Fig. 5A). Immediately after US exposure, the temperature started to increase. Under the US condition: frequency of 1.0 MHz, duty cycle of 5.2%, pulse repetition frequency of 20 Hz and $I_{SPPA.3}$ of 0.228 W/cm^2, the temperature increased slightly (approximately 28.5°C) and always remained less than about 32°C in the periocular area (Fig. 5B). However,

Table 1. Acoustic output level of ultrasounds about Sonitron 2000

Probe	Intensity (Indicated on the device)	Duty cycle	Pulse repetition frequency	Peak rarefactional acoustic pressure (MPa)	$I_{SPPA.3}$ (W/cm^2)	$I_{SPTA.3}$ (mW/cm^2)
6 mm	Low mode	5.2%	20 Hz	0.397	5.409	280.169
6 mm	Low mode	100%	continuous wave	0.425	5.982	5933.022
6 mm	High mode	5.2%	20 Hz	0.545	10.123	524.369
6 mm	High mode	100%	continuous wave	0.575	11.220	11128.540
3 mm	Low mode	5.2%	20 Hz	0.070	0.177	9.190
3 mm	Low mode	100%	continuous wave	0.065	0.155	154.032
3 mm	High mode	5.2%	20 Hz	0.083	0.228	11.791
3 mm	High mode	100%	continuous wave	0.062	0.156	154.484
FDA safety regulation					<28	<17

The frequency of this machine was fixed 1.0 MHz. $I_{SPPA.3}$ was less than 28 W/cm^2 under all conditions. Meanwhile $I_{SPTA.3}$ was less than 17 mW/cm^2 under only the condition of a duty cycle of 5.2% with 3 mm probe.

$I_{SPPA.3}$ = a derated spatial-peak pulse-average intensity; $I_{SPTA.3}$ = a derated spatial-peak temporal-average intensity.

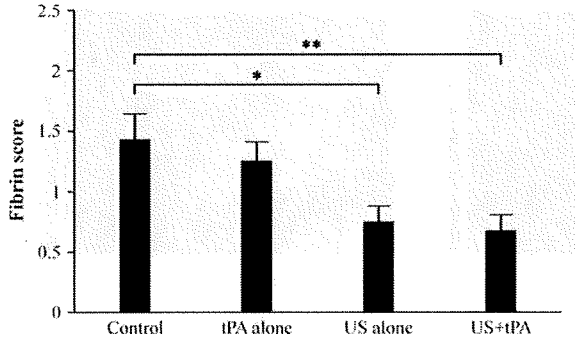

Fig. 3. Intracameral fibrin score on day 3. Intracameral fibrin clot decreased gradually over time and the average score on day 3. While the eyes that received subconjunctival tPA injection alone showed mild decrease of clots. There was no statistically significant difference from controls. In contrast, the eyes that received US alone or both tPA and US showed apparent decrease of clots (paired *t*-test, $*p < 0.05$, $**p < 0.01$).

under the US condition: frequency of 1.0 MHz, duty cycle of 100%, continuous wave mode and $I_{SPPA.3}$ of 0.156 W/cm^2, the temperature increased considerably (to about 34°C) more than the periocular area (Fig. 5C).

Histological findings. In immediate histological finding after YAG laser treatment, there was not any apparent damage in other ocular tissues including cornea and retina (Fig. 6). After US irradiation, the structure of the cornea was well preserved and neither inflammatory cell infiltration nor stromal edema was found. Retinal structure was also well preserved and neither inflammatory infiltrate nor hemorrhage was observed either (Fig. 7).

DISCUSSION

In this study, we found that US exposure significantly accelerated the disappearance of intracameral fibrin without causing any apparent damage. It is further important that this effect was accomplished within the range of safety condition.

Many reports show that US exposure accelerates fibrinolysis in vitro and combining US with various thrombolytic agents, *e.g.*, heparin sulfate, aspirin, urokinase type-plasminogen activator or tPA further accelerated fibrinolysis (Francis et al. 1992; Holland et al. 2008; Hong et al. 1990; Lauer et al. 1992; Tachibana 1992; Trübestein et al. 1976). In the present study, US exposure significantly enhanced fibrinolysis *in vitro* without thermal elevation; this effect was augmented by tPA. Although we cannot know the exact mechanism by which US accelerated fibrinolysis, most currently accepted or possible explanations are that US exposure changes the structure of clots and alters the drug distribution, resulting in deeper penetration into the clots by US, namely due to acoustic cavitations, bubble vibration, and their collapse (Datta et al. 2006; Francis et al. 1992; Hong et al. 1990; Lauer et al. 1992; Tachibana 1992; Trübestein et al. 1976). Of note, we have to interpret the results cautiously. In this study, we used borosilicate glass

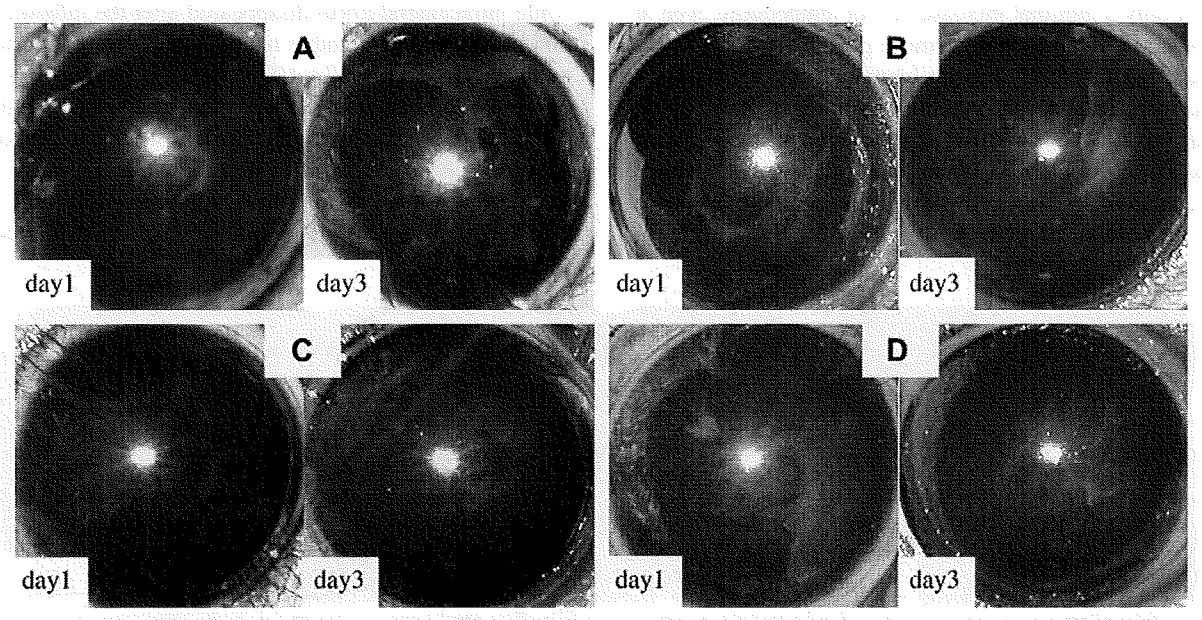

Fig. 4. Representative photograph of rat eyes after bleeding followed by treatment. Intracameral bleeding was induced by Nd:YAG laser shot on iris followed by subconjunctiva tPA injection and/or US exposure. Intracameral fibrin was scored on day 3. (A) Control. Fibrin clots decreased gradually. (B) US exposure alone. Fibrin clots was apparently decreased. (C) Subconjunctival tPA injection alone. Fibrin clots decreased gradually and there was no apparent difference from controls. (D) Subconjunctival tPA plus US exposure. Fibrin clots was significantly decreased and no clot was observed on day 3.

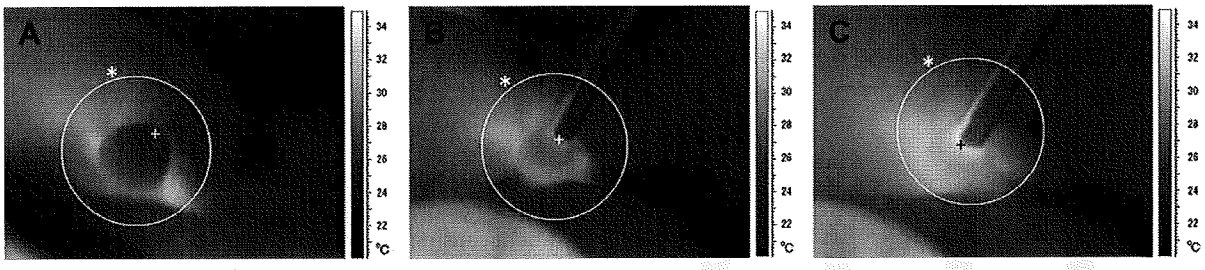

Fig. 5. The thermographic images of ultrasound-treated eye by an infrared thermography. Temperature was expressed as a pseudo-color. (A) Control. The highest temperature within the circle (denoted by an asterisk) was 31.9°C and the temperature of the spot + was 24.4°C. (B) US exposure for 5 min under the condition: frequency of 1.0 MHz, duty cycle of 5.2%, pulse repetition frequency of 20 Hz and $I_{SPPA.3}$ of 0.228 W/cm^2. The highest temperature within the circle (denoted by an asterisk) was 31.2°C and the temperature of the spot + was 28.5°C. (C) US exposure for 5 min under the condition: frequency of 1.0 MHz, duty cycle of 100%, continuous wave mode and $I_{SPPA.3}$ of 0.156 W/cm^2. The highest temperature within the circle (denoted by an asterisk) was the area of the spot +, which was 33.7°C.

tubes and that might have augmented ultrasound effect excessively. The unexpected reflection might have been involved in this phenomenon. However, it was unlikely that the present fibrinolysis was caused by thermal effect, because there was no change in temperature in the tube before and after ultrasound in this in vitro system even by the prolonged exposure (20 min). Importantly, the goal of our study is clinical application of US for intraocular fibrinolysis, which could be achieved in rat eyes. It requires further studies to elucidate the real mechanism of the present phenomenon.

Heating is a concern for tissue damage but it could accelerate clot-lysis on the other hand. Francis et al. (1992, 1995) reported that US exposure is associated with only a minimal increase of clot temperature even at 4 W/cm^2, which would be more potent than our conditions. In this study, the clot temperature *in vitro* shows less increase under the condition: frequency of 1.0 MHz, duty cycle of 5.2%, pulse repetition frequency of 20 Hz and $I_{SPPA.3}$of 10.123 W/cm^2 and the ocular surface temperature *in vivo* showed a minimal increase under the condition: frequency of 1.0 MHz, duty cycle of 5.2%, pulse repetition frequency of 20 Hz and $I_{SPPA.3}$ of 0.228 W/cm^2. Thus, it is likely that a nonthermal mechanism played a central role in our observations. Given the results of the *in vitro* study, it is understandable that intracameral fibrinolysis was accelerated by US exposure in rats. However, *in vivo* conditions are totally different from those *in vitro*.

In our previous study using the same model, there were various pro- or antifibrinolytic materials in the anterior chamber such as tPA and its inhibitor, unlike in vitro experiments (Sakamoto et al. 1999). Additionally, the intraocular environment is not stable and is strongly modulated by other factors. For example, if severe inflammation occurred, intracameral fibrin was easily formed while intracameral fibrin disappeared after the inflammation had gone. On the other hand, platelets were reported to be activated *in vitro* by US exposure (Chater and Williams 1977). Thus, it was of note that US exposure under the present condition caused fibrinolysis in the present study.

Under normal conditions, anterior chamber fluid is transparent and tPA is dominant over plasminogen

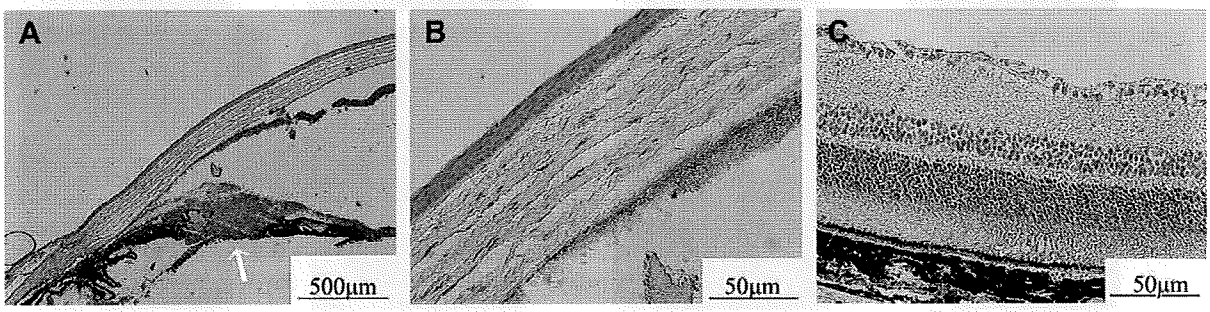

Fig. 6. Histologic photographs of rat eyes after YAG laser shot, before US exposure. (A) The only limited area of iris (arrow) was destroyed, called iridectomy hole, and 1/3 of the anterior chamber was filled with fibrin clot and red blood cells. (B) Fibrin clot and fibrin deposit were also found just beneath the corneal endothelium. There was not any apparent damage in other ocular tissues including cornea (B) and retina (C). Hematoxylin and eosin staining. Original magnification is (A) ×4, (B) ×40 and (C) ×40.

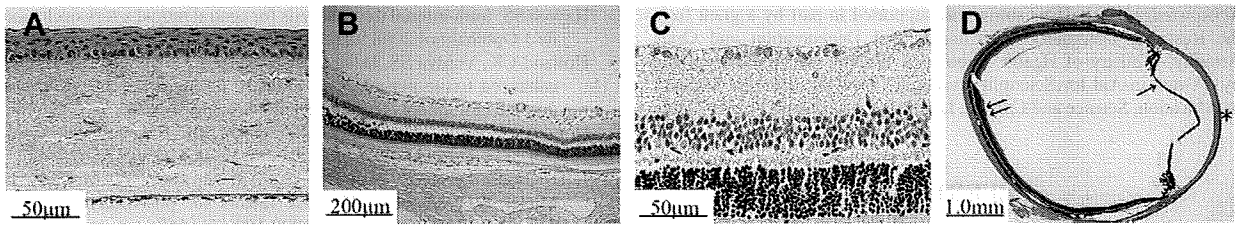

Fig. 7. Histologic photographs of rat eyes after US exposure. Original structure is well preserved and neither degeneration nor inflammation is found in cornea (A), retino-choroid (B) or retina (C). (D) The eyeball of the rat. Asterisk indicates cornea, arrow indicates iris and double arrow indicates retina. Hematoxylin and eosin staining. Original magnification is (A) ×40, (B) ×4, (C) ×40 and (D) ×2.

activator inhibitor (Fukushima et al. 1989). Fibrinolytic materials such as tPA were also assumed to be dominant over inhibitors after iris bleeding in this model because intracameral fibrin decreased gradually without any treatment. Therefore, US treatment accelerated intracameral fibrinolysis associated with tPA to some extent. Further study is necessary to clarify the mechanism in more detail.

Unlike the *in vitro* study, the additional injection of tPA to US exposure did not augment intracameral fibrinolysis. In this study, we did not use a direct intraocular injection of tPA because the intraocular injection itself could influence the intraocular fibrinolytic system. Instead, tPA was injected into subconjunctiva to avoid this destabilizing factor. As a result, it could not further enhance fibrinolysis. It was possible that subconjunctival tPA was degraded or did not penetrate the anterior chamber and thus active tPA might not be present sufficiently in the anterior chamber. An improved drug delivery system would be necessary.

US is a routine diagnostic procedure for ocular diseases and therapeutic application to glaucoma and intraocular tumor has already reported (Coleman et al. 1985, 1988). US is also believed to be a promising therapeutic alternative by several experimental studies (Sonoda et al. 2006; Yamashita et al. 2007; White et al. 2008; Zderic et al. 2004). However, US has still not been accepted for clinical use in most of ocular diseases including intraocular hemorrhage and vascular disorders.

This is not only because therapeutic value has not been well developed but there have also been concerns about its potentially harmful effects (Brown 1984). For example, the corneal endothelium *in vitro* was damaged by US exposure (Saito et al. 1999).

As this study reveals, the effects of US were influenced by various factors. Among them, the duty ratio was the strongest factor inducing a possible harmful event. In our *in vivo* study, the surface temperature of rat eyes increased to about 34 °C with the following conditions: frequency of 1.0 MHz and duty cycle of 100%, which was higher than periocular area while the surface temperature was not changed so much with a duty cycle of 5.2%. It is difficult to conclude that the present treatment is not harmless; however, it should be noted that a beneficial effect, intracameral fibrinolysis, could be obtained without causing a harmful event, histologically or clinically. Obviously, a human eye is much bigger than a rat eye and careful setting of US conditions would enable the therapeutic value of this treatment to be established.

There are many ocular diseases to which this treatment is potentially applicable. Of them, RAO is a good candidate. As is often quoted, a disease without any treatment has many treatments and RAO is a good example. The onset-to-treatment interval is the most critical issue for the successful treatment of RAO because longer periods of tissue ischemia result in irreversible retinal damage and permanent dysfunction. In a study with primates, the interval should be less than a few hours (Hayreh 2008; Hayreh et al. 2004). In comparison to surgery or intraocular injection, the present treatment is less invasive and does not need specific preparations for treatment (*e.g.*, disinfection treatment), which might waste precious time for effective treatment. Furthermore, US exposure might also be effective for removing cholesterol or calcium emboli because US can induce mechanical vibration. Considering these benefits, the present treatment should be worthy of study in a future clinical setting, although there are still many issues to be solved.

It is of note that our animal model is not that of retinal artery occlusion. To our knowledge, there is no reproducible animal model of retinal artery occlusion that is suitable for evaluating therapies. In contrast, the present model is suitable for studying the effect of intervention on intraocular fibrinolysis *in vivo*. This would give us the important information to develop a new treatment of retinal artery occlusion.

In conclusion, the present study shows that US exposure from outside can accelerate intraocular fibrinolysis. A beneficial effect was obtained without causing apparent damage. The US power was within the safety range of FDA regulations. Therefore, there might be more suitable ocular conditions for US treatment than given in the examples above. The present results could provide basic evidence to justify US treatment for ocular diseases related to fibrin formation.

Acknowledgements—This study was supported in part by a grant from the Research Committee on Chorioretinal Degeneration and Optic Atrophy, Ministry of Health, Labor and Welfare (Dr. Sakamoto) and by a Grant-in-Aid for Scientific Research 19659452 from the Ministry of Education, Science and Culture, Japanese Government, Tokyo, Japan.

REFERENCES

Akassoglou K, Adams RA, Bauer J, Mercado P, Tseveleki V, Lassmann H, Probert L, Strickland S. Fibrin depletion decreases inflammation and delays the onset of demyelination in a tumor necrosis factor transgenic mouse model for multiple sclerosis. Proc Natl Acad Sci U S A 2004;101:6698–6703.

Alexandrov AV, Molina CA, Grotta JC, Garami Z, Ford SR, Alvarez-Sabin J, Montaner J, Saqqur M, Demchuk AM, Moye LA, Hill MD, Wojner AW. Ultrasound-enhanced systemic thrombolysis for acute ischemic stroke. N Engl J Med 2004;351:2170–2178.

Brown BS. How safe is diagnostic ultrasonography? Can Med Assoc J 1984;131:307–311.

Chater BV, Williams AR. Platelet aggregation induced *in vitro* by therapeutic ultrasound. Thromb Haemost 1977;38:640–651.

Cohen MG, Tuero E, Bluguermann J, Kevorkian R, Berrocal DH, Carlevaro O, Picabea E, Hudson MP, Siegel RJ, Douthat L, Greenbaum AB, Echt D, Weaver WD, Grinfeld LR. Transcutaneous ultrasound-facilitated coronary thrombolysis during acute myocardial infarction. Am J Cardiol 2003;92:454–457.

Coleman DJ, Lizzi FL, Driller J, Rosado AL, Burgess SE, Torpey JH, Smith ME, Silverman RH, Yablonski ME, Chang S, Rondeau MJ. Therapeutic ultrasound in the treatment of glaucoma. II. Clinical applications. Ophthalmology 1985;92:347–353.

Coleman DJ, Silverman RH, Iwamoto T, Lizzi FL, Rondeau MJ, Driller J, Rosado A, Abramson DH, Ellsworth RM. Histopathologic effects of ultrasonically induced hyperthermia in intraocular malignant melanoma. Ophthalmology 1988;95:970–981.

Daffertshofer M, Gass A, Ringleb P, Sitzer M, Sliwka U, Els T, Sedlaczek O, Koroshetz WJ, Hennerici MG. Transcranial low-frequency ultrasound-mediated thrombolysis in brain ischemia: Increased risk of hemorrhage with combined ultrasound and tissue plasminogen activator: Results of a phase II clinical trial. Stroke 2005;36:1441–1446.

Datta S, Coussios C-C, McAdory LE, Tan J, Porter T, de Courten-Myers G, Holland CK. Correlation of cavitation with ultrasound enhancement of thrombolysis. Ultrasound Med Biol 2006;32:1257–1267.

Drake MV. Neodymium:YAG laser iridotomy. Surv Ophthalmol 1987;32:171–177.

Feltgen N, Neubauer A, Jurklies B, Schmoor C, Schmidt D, Wanke J, Maier-Lenz H, Schumacher M. Multicenter study of the European Assessment Group for Lysis in the Eye (EAGLE) for the treatment of central retinal artery occlusion: Design issues and implications. EAGLE Study report no. 1: EAGLE Study report no. 1. Graefes Arch Clin Exp Ophthalmol 2006;244:950–956.

Francis CW, Onundarson PT, Carstensen EL, Blinc A, Meltzer RS, Schwarz K, Marder VJ. Enhancement of fibrinolysis *in vitro* by ultrasound. J Clin Invest 1992;90:2063–2068.

Francis CW, Blinc A, Lee S, Cox C. Ultrasound accelerates transport of recombinant tissue plasminogen activator into clots. Ultrasound Med Biol 1995;21:419–424.

Frenkel V, Oberoi J, Stone MJ, Park M, Deng C, Wood BJ, Neeman ZM III, Li KC. Pulsed high-intensity focused ultrasound enhances thrombolysis in an *in vitro* model. Radiology 2006;239:86–93.

Fukushima M, Nakashima Y, Sueishi K. Thrombin enhances release of tissue plasminogen activator from bovine corneal endothelial cells. Invest Ophthalmol Vis Sci 1989;30:1576–1583.

Garcia-Arumi J, Martinez-Castillo V, Boixadera A, Fonollosa A, Corcostegui B. Surgical embolus removal in retinal artery occlusion. Br J Ophthalmol 2006;90:1252–1255.

Hayreh SS, Zimmerman MB, Kimura A, Sanon A. Central retinal artery occlusion. Retinal survival time. Exp Eye Res 2004;78:723–736.

Hayreh SS. Intra-arterial thrombolysis for central retinal artery occlusion. Br J Ophthalmol 2008;92:585–587.

Holland CK, Vaidya SS, Datta S, Coussios C-C, Shaw GJ. Ultrasound-enhanced tissue plasminogen activator thrombolysis in an *in vitro* porcine clot model. Thromb Res 2008;121:663–673.

Hong AS, Chae JS, Dubin SB, Lee S, Fishbein MC, Siegel RJ. Ultrasonic clot disruption: An *in vitro* study. Am Heart J 1990;120:418–422.

Jaffe GJ, Schwartz D, Han DP, Gottlieb M, Hartz A, McCarty D, Mieler WF, Abrams GW. Risk factors for postvitrectomy fibrin formation. Am J Ophthalmol 1990;109:661–667.

Kattah JC, Wang DZ, Reddy C. Intravenous recombinant tissue-type plasminogen activator thrombolysis in treatment of central retinal artery occlusion. Arch Ophthalmol 2002;120:1234–1236.

Lauer CG, Burge R, Tang DB, Bass BG, Gomez ER, Alving BM. Effect of ultrasound on tissue-type plasminogen activator-induced thrombolysis. Circulation 1992;86:1257–1264.

McDonald HR, Schatz H, Johnson RN. Postoperative intraocular fibrin formation is a potentially disastrous complication of vitrectomy surgery. Retina 1990;10:317–318.

Noble J, Weizblit N, Baerlocher MO, Eng KT. Intra-arterial thrombolysis for central retinal artery occlusion: A systematic review. Br J Ophthalmol 2008;92:588–593.

Opremcak E, Rehmar AJ, Ridenour CD, Borkowski LM, Kelley JK. Restoration of retinal blood flow *via* translumenal Nd:YAG embolysis/embolectomy (TYL/E) for central and branch retinal artery occlusion. Retina 2008;28:226–235.

Pfaffenberger S, Devcic-Kuhar B, Kastl SP, Huber K, Maurer G, Wojta J, Gottsauner-Wolf M. Ultrasound thrombolysis. Thromb Haemost 2005;94:26–36.

Richard G, Lerche RC, Knospe V, Zeumer H. Treatment of retinal arterial occlusion with local fibrinolysis using recombinant tissue plasminogen activator. Ophthalmology 1999;106:768–773.

Saito K, Miyake K, McNeil PL, Kato K, Yago K, Sugai N. Plasma membrane disruption underlies injury of the corneal endothelium by ultrasound. Exp Eye Res 1999;68:431–437.

Sakamoto T, Oshima Y, Nakagawa K, Ishibashi T, Inomata H, Sueishi K. Target gene transfer of tissue plasminogen activator to cornea by electric pulse inhibits intracameral fibrin formation and corneal cloudiness. Hum Gene Ther 1999;10:2551–2557.

Sonoda S, Tachibana K, Uchino E, Okubo A, Yamamoto M, Sakoda K, Hisatomi T, Sonoda KH, Negishi Y, Izumi Y, Takao S, Sakamoto T. Gene transfer to corneal epithelium and keratocytes mediated by ultrasound with microbubbles. Invest Ophthalmol Vis Sci 2006;47:558–564.

Tachibana K. Enhancement of fibrinolysis with ultrasound energy. J Vasc Intervent Radiol 1992;3:299–303.

Tachibana K, Tachibana S. Albumin microbubble echo-contrast material as an enhancer for ultrasound accelerated thrombolysis. Circulation 1995;92:1148–1150.

Tachibana K, Tachibana S. Prototype therapeutic ultrasound emitting catheter for accelerating thrombolysis. J Ultrasound Med 1997;16:529–535.

Tomey KF, Traverso CE, Shammas IV. Neodymium-YAG laser iridotomy in the treatment and prevention of angle closure glaucoma. A review of 373 eyes. Arch Ophthalmol 1987;105:476–481.

Toth CA, Morse LS, Hjelmeland LM, Landers MB III. Fibrin directs early retinal damage after experimental subretinal hemorrhage. Arch Ophthalmol 1991;109:723–729.

Trubestein G, Engel C, Etzel F, Sobbe A, Cremer H, Stumpff U. Thrombolysis by ultrasound. Clin Sci Mol Med Suppl 1976;3:697s–698s.

Vine AK, Samama MM. The role of abnormalities in the anticoagulant and fibrinolytic systems in retinal vascular occlusions. Surv Ophthalmol 1993;37:283–292.

Weber J, Remonda L, Mattle HP, Koerner U, Baumgartner RW, Sturzenegger M, Ozdoba C, Koerner F, Schroth G. Selective intra-arterial fibrinolysis of acute central retinal artery occlusion. Stroke 1998;29:2076–2079.

White WM, Makin IR, Slayton MH, Barthe PG, Gliklich R. Selective transcutaneous delivery of energy to porcine soft tissues using Intense Ultrasound (IUS). Lasers Surg Med 2008;40:67–75.

Yamamoto T, Kamei M, Kunavisarut P, Suzuki M, Tano Y. Increased retinal toxicity of intravitreal tissue plasminogen activator in a central

retinal vein occlusion model. Graefes Arch Clin Exp Ophthalmol 2008;246:509–514.

Yamashita T, Sonoda S, Suzuki R, Arimura N, Tachibana K, Maruyama K, Sakamoto T. A novel bubble liposome and ultrasound-mediated gene transfer to ocular surface: RC-1 cells in vitro and conjunctiva *in vivo*. Exp Eye Res 2007;85:741–748.

Yoeruek E, Spitzer MS, Tatar O, Biedermann T, Grisanti S, Luke M, Bartz-Schmidt KU, Szurman P. Toxic effects of recombinant tissue plasminogen activator on cultured human corneal endothelial cells. Invest Ophthalmol Vis. Sci 2008;49:1392–1397.

Zderic V, Clark JI, Vaezy S. Drug delivery into the eye with the use of ultrasound. J Ultrasound Med 2004;23:1349–1359.

THE JOURNAL OF BIOLOGICAL CHEMISTRY VOL. 284, NO. 14, pp. 9147–9152, April 3, 2009

Characterization of N-terminal Structure of TLR2-activating Lipoprotein in *Staphylococcus aureus*[*]

Received for publication, January 21, 2009 Published, JBC Papers in Press, February 13, 2009, DOI 10.1074/jbc.M900429200

Kazuki Tawaratsumida[‡], Maiko Furuyashiki[§], Mami Katsumoto[¶], Yukari Fujimoto[¶], Koichi Fukase[¶], Yasuo Suda[‡], and Masahito Hashimoto[‡1]

From the [‡]Department of Nanostructure and Advanced Materials and [§]Venture Business Laboratory, Kagoshima University, Korimoto 1-21-40, Kagoshima 890-0065 and the [¶]Department of Chemistry, Graduate School of Science, Osaka University, Toyonaka, Osaka 560-0043, Japan

Staphylococcus aureus **is known to activate mammalian immune cells through Toll-like receptor 2 (TLR2). We recently demonstrated that a lipoprotein fraction obtained from *S. aureus* by Triton X-114 phase partitioning is a potent activator of TLR2. In this study, we separated TLR2-activating lipoproteins expressed in *S. aureus* and characterized an N-terminal structure. The lipoprotein fraction of *S. aureus* was prepared by glass bead disruption followed by Triton X-114 phase partitioning. The TLR2-activating molecules were mainly detected in the mass range of 30–35 kDa. Seven lipoproteins were identified by the mass spectra of their tryptic digests. Among them, three lipoproteins were separated by preparative SDS-PAGE and proved to activate TLR2. After digestion with trypsin in the presence of sodium deoxycholate, the N terminus of the lipopeptide was isolated from lipoprotein SAOUHSC_02699 by normal phase high pressure liquid chromatography and characterized as an *S*-(diacyloxypropyl)cystein-containing peptide using tandem mass spectra. The synthetic lipopeptide counterpart also stimulated the cells via TLR2. These results showed that the diacylated lipoprotein from *S. aureus* acts as a TLR2 ligand in mammalian cells.**

Bacterial infection is one of the major causes of death. *Staphylococcus aureus*, the most common Gram-positive pathogen, is a major source of mortality in medical facilities (1). The pathogen causes various infectious diseases, including sepsis, endocarditis, and pneumonia. During the infection, *S. aureus* activates cells and evokes serious inflammation in the host. TLR2 [2] has been shown to play a crucial role in the host response to *S. aureus* (2). However, a detailed understanding of the molecular components that interact with TLR2 in *S. aureus* cells has not yet been obtained. One of the reported TLR2 ligands was peptidoglycan (PGN) (3), a cell wall component of most bacteria. However, Travassos *et al.* (4) recently showed that PGN from several bacteria that were highly purified by removal of lipoproteins or lipoteichoic acid (LTA) were not detected by TLR2. Moreover, the minimal active components of the PGN, muramyl dipeptide and desmuramyl dipeptide (γ-D-glutamyl diaminopimelic acid), were determined to be ligands of the intracellular innate immune receptor Nod2/Nod1 (5, 6), suggesting that PGN is not a ligand of TLR2. Another candidate of TLR2-activating ligands is LTA, a cell surface glycoconjugate of Gram-positive bacteria (3). Morath *et al.* (7) reported that LTA from *S. aureus* is a potent stimulator of cytokine release, whereas our group demonstrated that LTA from enterococci, also a major Gram-positive pathogen, has no cytokine-producing activity (8, 9). Furthermore, Han *et al.* (10) showed that LTA from pneumococci is 100-fold less potent than staphylococcal LTA. These observations suggested that LTA is not a common ligand of TLR2 in Gram-positive pathogens.

We also found that the enterococcal LTA fraction contains some contaminants other than LTA and that these components activate immune cells through TLR2 (8, 11). However, their structures were not identified at that time. TLR2 is known to be a predominant receptor for lipoproteins derived from various bacteria. We have previously shown that the lipoprotein-containing fraction from *S. aureus* stimulates activation of immune cells through TLR2 (12). Recently, Stoll *et al.* (13) constructed a lipoprotein diacylglycerol transferase deletion (Δ*lgt*) mutant of *S. aureus*, which is unable to carry out lipid modification of prelipoproteins. It was demonstrated that the mutant completely lacks palmitate-labeled lipoproteins and that its cells and crude lysate induce much less proinflammatory cytokines than the wild type. Bubeck *et al.* (14) also reported that an *S. aureus* variant that lacks lipoproteins is able to escape immune recognition and cause lethal infections. Furthermore, we showed that the activities of an LTA fraction derived from a Δ*lgt* mutant are largely decreased when compared with those from the same fraction of the wild type (15). These results suggest that the lipoproteins in *S. aureus* appear to be the TLR2 ligand for the immune system. In the present study, we separated lipoproteins from *S. aureus* and elucidated the TLR2-activating structure.

EXPERIMENTAL PROCEDURES

Bacterial Strain and Bacterial Components—*S. aureus* SA113, a restriction-deficient mutant of NCTC8325 (16), was cultured in brain heart infusion broth (Eiken, Tokyo, Japan) at 37 °C for 6 h with constant shaking in a culture bag (CB20-1, Fujimori Kogyo Co., Ltd., Tokyo, Japan) before being harvested by cen-

* This work was supported by a research grant from The Uehara Memorial Foundation.

[1] To whom correspondence should be addressed. Tel.:/Fax: 81-99-285-7742. E-mail: hassy@eng.kagoshima-u.ac.jp.

[2] The abbreviations used are: TLR, Toll-like receptor; mTLR2, murine TLR2; LTA, lipoteichoic acid; MALDI-TOF-MS, matrix-assisted laser desorption ionization-time of flight mass spectrometry; MS/MS, tandem mass spectrometry; PBMC, peripheral blood mononuclear cell; PGN, peptidoglycan; HPLC, high pressure liquid chromatography; TNF, tumor necrosis factor.

trifugation (5,000 × *g* for 15 min at 4 °C). The membrane fraction was prepared by bead disruption of the cells as described (13). The lipoprotein fraction was obtained by Triton X-114 phase partitioning of the membrane fraction as described (17) and was designated as Sa-M-TX.

FSL-1, a synthetic diacylated lipopeptide, was purchased from EMC microcollections (Tübingen, Germany). *Escherichia coli* O55:B5 lipopolysaccharide (Sigma-Aldrich) was further purified by sodium deoxycholate reextraction as described (18). SAOUHSC_02699 di-*O*-palmitoyl (Pam_2) lipopeptide 10-mer (Pam_2CGNNSSKDKDG) and Pam_2CSK_4 were synthesized in our laboratory. The synthetic details will be described elsewhere.

Separations of Proteins—Analytical SDS-PAGE was performed by the Tris-glycine method (19) using a mini PAGE chamber AE-6530 and an AE-8450 power supply (Atto Corp., Tokyo, Japan) with a 12.5% gel. Proteinous materials were visualized by silver or Coomassie Brilliant Blue staining, and visualization of acidic materials, such as LTA, was performed by Alcian blue staining.

Proteins eluting between 25 and 40 kDa in the analytical SDS-PAGE were separated using a preparative electrophoresis apparatus, AE-6750 (Atto Corp.), according to the manufacturer's instructions. The eluates were analyzed by SDS-PAGE and subjected to acetone precipitation to remove any contaminating SDS. The precipitates were dissolved in 20 mM octylglucoside. The concentration of lipoprotein was estimated by SDS-PAGE with silver staining and adjusted to 10 μg/ml.

Monocyte Western Blotting—Monocyte Western blotting was carried out by the method described previously (20). Briefly, stimuli were separated by SDS-PAGE, and the resolved stimuli in the gel were transblotted to a nitrocellulose membrane by the method of Towbin *et al.* (21) using an AE-6677 semidry blotting apparatus (Atto Corp.). The membrane of each lane was cut into 4-mm strips, and each strip was separately dissolved in dimethyl sulfoxide. The solution was poured into phosphate-buffered saline to precipitate stimuli-coated particles, which consist of stimuli and nitrocellulose. After washing three times with phosphate-buffered saline, the particle suspension in assay medium was applied to a luciferase assay using the Ba/mTLR2 cells described below.

Mass Spectrometry—Mass spectra were obtained by matrix-assisted laser desorption ionization-time of flight mass spectrometry (MALDI-TOF-MS) with an Axima QIT TOF mass spectrometer (Shimadzu, Kyoto, Japan) equipped with a nitrogen 337 nm laser. 2,5-Dihydroxybenzoic acid was used as the matrix at a concentration of 10 mg/ml in aqueous 50% acetonitrile containing 0.1% trifluoroacetic acid. Peptides were analyzed in positive and reflectron mode. Tandem mass (MS/MS) spectra were obtained using argon as a collision gas.

Identification of Lipoproteins and Lipopeptides—The proteins that were separated by analytical SDS-PAGE were digested with trypsin as described previously (22). The peptides were analyzed by MALDI-TOF-MS and identified by a data base (the National Center for Biotechnology Information nonredundant protein data base) search using the MASCOT software from Matrix Science (23). The proteins were designated

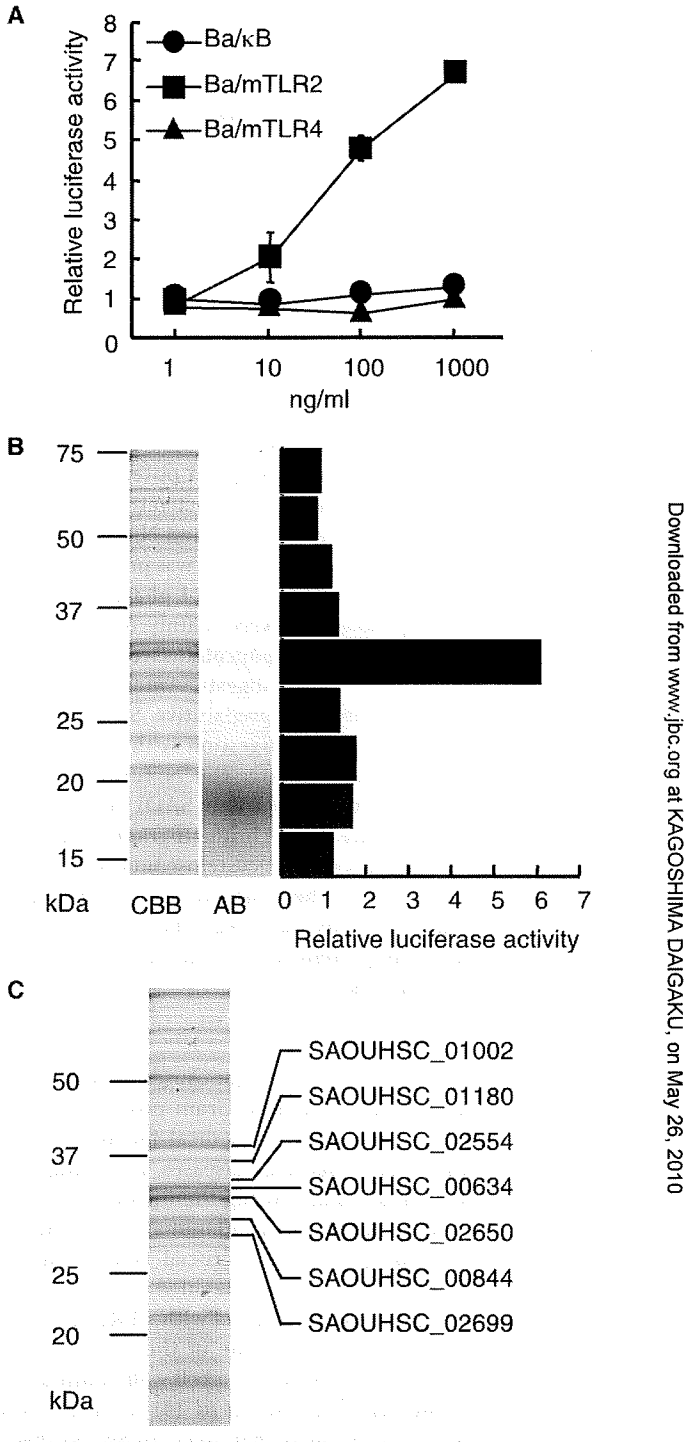

FIGURE 1. **Identification of lipoproteins in *S. aureus*.** *A*, the NF-κB activation induced by Sa-M-TX in Ba/κB, Ba/mTLR2, or Ba/mTLR4/mMD-2 cells for 4 h was measured with a luciferase assay. The results are shown as relative luciferase activity, which was determined as the ratio of stimulated to nonstimulated activity. The data represent the mean ± S.E. obtained from three independent experiments. *B*, SDS-PAGE profiles of Sa-M-TX and separation of TLR2-activating components in Sa-M-TX. The gels were separated with 12.5% gel and visualized by Coomassie Brilliant Blue (*CBB*) or Alcian blue (*AB*). NF-κB activation was detected by monocyte Western blotting using a luciferase assay in Ba/mTLR2 cells. The results are shown as relative luciferase activity, which was determined as the ratio of stimulated to nonstimulated activity. *C*, identification of lipoproteins in Sa-M-TX. Each protein were separated with 12.5% gel and identified by in-gel tryptic digestion followed by mass analysis.

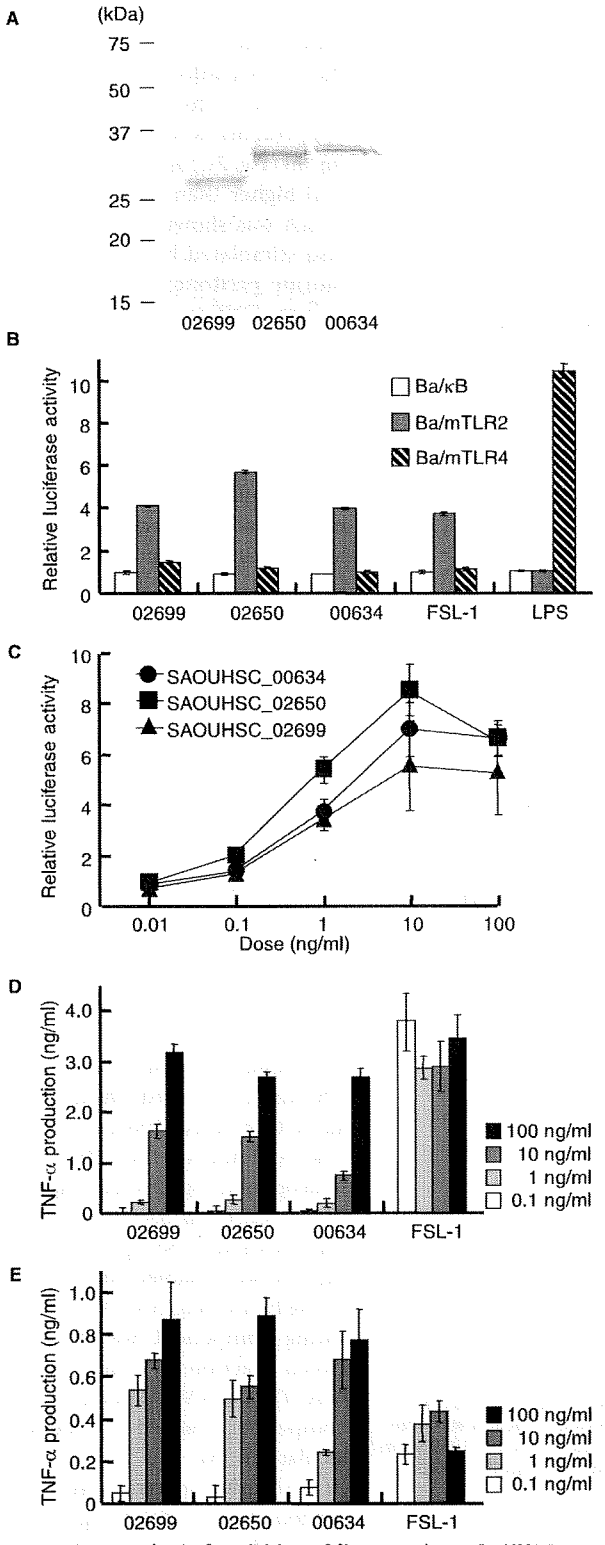

FIGURE 2. **Immunological activities of lipoproteins, SAOUHSC_02699, -02650, and -00634 separated by preparative SDS-PAGE using 12.5% gel.** *A*, SDS-PAGE profile of lipoproteins. They were separated in 12.5% gel and visualized by silver staining. *B*, the NF-κB activation induced by 1 ng/ml of the lipoprotein, 0.1 ng/ml FSL-1, and 10 ng/ml lipopolysaccharide (*LPS*) in Ba/κB, Ba/mTLR2, or Ba/mTLR4/mMD-2 cells. *C*, dose-dependent NF-κB activation induced by lipoproteins in Ba/mTLR2 cells. The cells were incubated with stimuli for 4 h. NF-κB activation was measured with a luciferase assay. The results are shown as relative luciferase activity, which was determined as the ratio of stimulated to nonstimulated activity. The data represent the mean ± S.E. obtained from three independent experiments. *D*, TNF-α production induced by the lipoprotein in human PBMC. *E*, TNF-α production induced by the lipoprotein in murine peritoneal exudate cells. The levels of TNF-α in the culture supernatants of the cells incubated with the indicated concentration of the stimuli for 4 h were measured by enzyme-linked immunosorbent assay. The data represent the mean ± S.E. obtained from three independent experiments.

by the locus tags for the genome of *S. aureus* NCTC8325, which is the parent strain of SA113 (16).

To isolate the N-terminal lipopeptide, the lipoprotein fraction was subjected to phase transfer surfactant-aided trypsin digestion (24). The tryptic digest was subjected to HPLC using a normal phase Daisopak SP-120-5-SIL-P column (250 × 4.6 mm, DAISO, Co., Ltd., Osaka, Japan). The digests were eluted using a gradient program (solvent A, chloroform, methanol, water = 65/20/3, v/v/v; solvent B, chloroform, methanol, water = 65/40/3, v/v/v) at a flow rate of 1.0 ml/min and were fractionated into 1-ml portions. The N-terminal lipopeptide was detected using a luciferase assay. The purified lipopeptide was characterized by MALDI-TOF-MS.

Luciferase Assay—Ba/F3 cells that stably expressed p55IgκLuc, an NF-κB/DNA binding activity-dependent luciferase reporter construct (Ba/κB), murine TLR2 and the p55IgκLuc reporter construct (Ba/mTLR2), and murine TLR4/MD-2 and the p55IgκLuc reporter construct (Ba/mTLR4/mMD-2) were kindly provided by Prof. K. Miyake (Institute of Medical Science, University of Tokyo, Japan). The NF-κB-dependent luciferase activity in these cells was determined as described previously (12).

Cytokine Assay—Eight-week-old male BALB/c mice were obtained from Kyudo (Kumamoto, Japan). The animals received humane care in accordance with our institutional guidelines and the legal requirements of Japan. Stimulation of thioglycolate-elicited peripheral exudate cells and Histopaque-separated human peritoneal blood mononuclear cells (PBMC) from a healthy donor (M. F.) and a cytokine assay for secreted murine or human TNF-α were performed as described (15).

RESULTS

Identification of Lipoproteins in S. aureus—The lipoprotein fraction was obtained from *S. aureus* cells using glass bead disruption followed by Triton X-114 phase partitioning. Four mg of the lipoprotein fraction (Sa-M-TX) were obtained from 10 liters of bacterial cell culture. Sa-M-TX activated murine TLR2 expressing cells (Ba/mTLR2) at 10 ng/ml but not murine TLR4 and MD-2 expressing Ba/mTLR4/mMD-2 cells or the negative control Ba/κB cells (Fig. 1*A*). The SDS-PAGE profile of Sa-M-TX showed that it contained Coomassie Brilliant Blue (*CBB*)-positive proteins and Alcian blue (*AB*)-positive components (Fig. 1*B*). The active molecules in Sa-M-TX were analyzed by monocyte Western blotting. TLR2-mediated NF-κB activation was strongly detected in a molecular mass range of 30–35 kDa (Fig. 1*B*). Thus, we subjected the Sa-M-TX proteins with molecular masses of around 30–35 kDa to in-gel tryptic digestion. At least seven lipoproteins, SAOUHSC_00634, -00844, -01002, -01180, -02554, -02650, and -02699, were identified by a combination of peptide mass fingerprinting and MS/MS spectra (Fig. 1*C*).

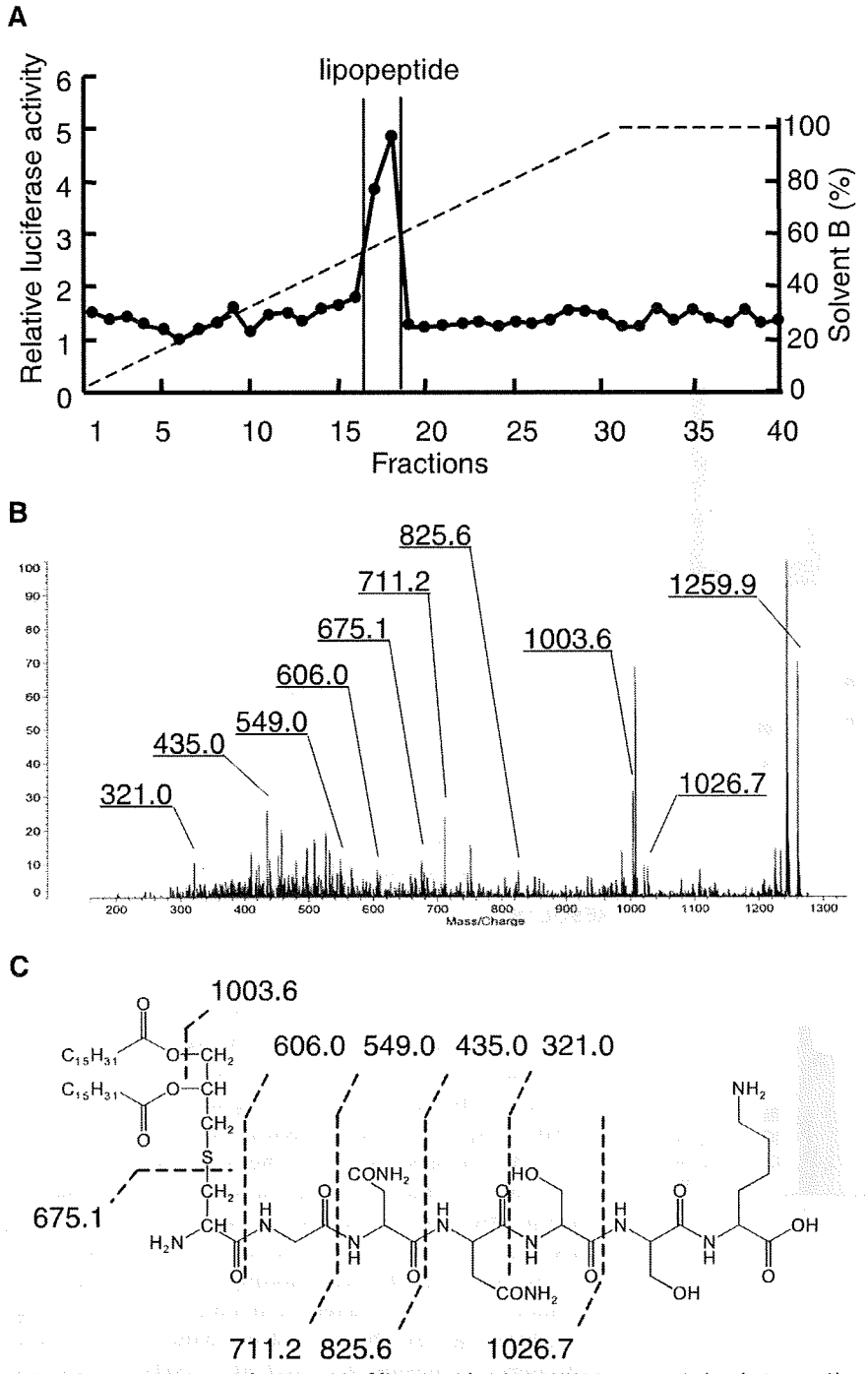

FIGURE 3. **Characterization of the N-terminal lipopeptide of SAOUHSC_02699.** *A*, the elution profile of a tryptic digest of SAOUHSC_02699 using normal phase HPLC. The NF-κB activation of the fraction was determined using Ba/mTLR2 cells. *B*, the MS/MS spectrum of the lipopeptide. The precursor ion at *m/z* 1259.9 was decomposed using collision-induced dissociation (CID) mode. *C*, the structure of the lipopeptide. Interpretations of the fragment ions in the MS/MS spectra are indicated in the structure.

Lipoprotein Immunological Activities—The lipoproteins were separated by preparative SDS-PAGE using a 12.5% gel. Among seven identified lipoproteins, we could separate three lipoproteins, SAOUHSC_02699, -02650, and -00634 (Fig. 2*A*). About 1 μg of each lipoprotein were obtained from 250 μg of Sa-M-TX. The TLR2-dependent activities of the lipoproteins were detected by NF-κB activation in TLR-expressing cells. All lipoproteins induced NF-κB activation in Ba/mTLR2 cells but not in Ba/mTLR4/mMD-2 or Ba/κB cells (Fig. 2*B*). The activities of the lipoproteins were observed at 0.1 ng/ml (Fig. 2*C*) and were about 100-fold higher than that of Sa-M-TX, which was shown in Fig. 1*A*. They also stimulated human PBMC and murine peritoneal exudate cells to induce TNF-α dose dependently (Fig. 2, *D* and *E*). The other four lipoproteins could not be analyzed because of the low content in Sa-M-TX.

The N-terminal Structure of S. aureus Lipoprotein—Because the minimal active structure of bacterial lipoproteins is reported to be N-terminal acylated *S*-(2,3-dihydroxypropyl)cysteine-containing lipopeptide (25), the N-terminal structure of *S. aureus* lipoprotein was investigated. We attempted to separate N-terminal lipopeptides from three separated lipoproteins by conventional tryptic digestion followed by reverse or normal phase HPLC separation. Although active components were eluted, no lipopeptides were detected by mass spectrometry. This may have been caused by insufficient digestion of the N-terminal moiety of the lipopeptides, probably because of poor solubility or micelle formation. Therefore, we used phase transfer surfactant-aided trypsin digestion (24) to improve the efficiency of hydrophobic lipoprotein digestion. The lipoprotein SAOUHSC_02699 was thus able to be digested, and the digests were subjected to normal phase HPLC (Fig. 3*A*). A TLR2-activating component was found between fractions 17 and 18. The MALDI-TOF-MS spectra of the component showed a pseudomolecular ion $[M+H]^+$ at *m/z* 1259.9. In the MS/MS spectra of the precursor ion at *m/z* 1259.9 (Fig. 3, *B* and *C*), C-terminal y ions were observed at *m/z* 606.0, 549.0, 435.0, and 321.0, which agreed with the N-terminal sequence of SAOUHSC_02699, GNNSSK. The ions at *m/z* 1026.7, 825.6, and 711.2 correspond to b ions of an *S*-(dipalmitoyloxypropyl)-cysteine-containing peptide. The ion at *m/z* 675.1 represents dehydroalanyl GNNSSK, which is formed by β-elimination of the 2,3-dipalmitoyloxypropylthio group. These results prove

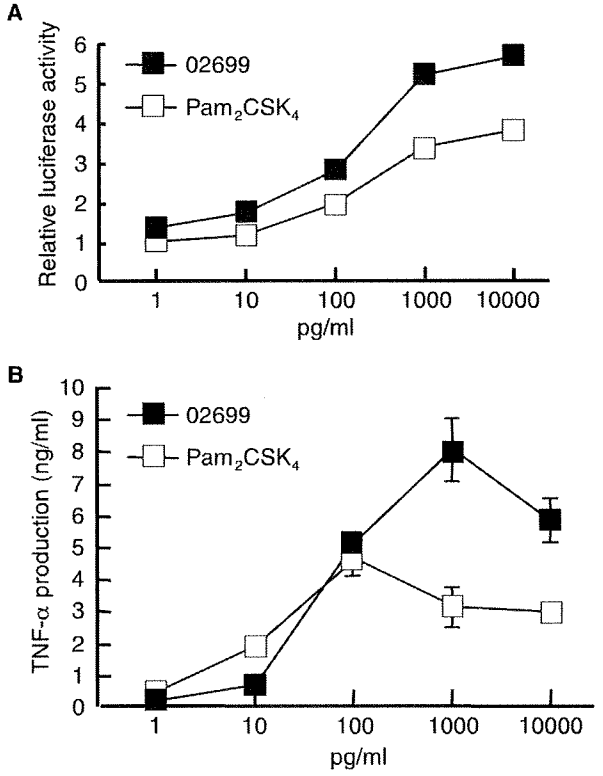

FIGURE 4. **Immunological activities of a synthetic lipopeptide of SAOUHSC_02699.** *A*, NF-κB activation induced by the indicated doses of lipopeptide in Ba/mTLR2 cells for 4 h was measured with a luciferase assay. The results are shown as relative luciferase activity, which was determined as the ratio of stimulated to nonstimulated activity. The data represent the mean ± S.E. obtained from three independent experiments. *B*, TNF-α production induced by the lipoprotein in human PBMC. The levels of TNF-α in the culture supernatants of the cells incubated with the indicated concentration of the stimuli for 4 h were measured by enzyme-linked immunosorbent assay. The data represent the mean ± S.E. obtained from three independent experiments.

that the N-terminal structure of SAOUHSC_02699 is a diacyl-type lipoprotein. The synthetic counterpart of its N-terminal lipopeptide 10-mer stimulated TLR2-dependent NF-κB activation in Ba/mTLR2 cells and TNF-α induction in PBMC (Fig. 4). The lipoprotein SAOUHSC_00634 and -02650 were also subjected to the phase transfer surfactant-aided trypsin digestion. Although active components were eluted from HPLC, no spectra corresponding to lipopeptide were obtained, suggesting that further improvement is required for complete digestion of some lipoproteins.

DISCUSSION

S. aureus is known to activate TLR2, but the principal molecule responsible for this activity has not been proven. In this study, we identified several lipoproteins including SAOUHSC_01002, -01180, -02554, -00634, -02650, -00844, and -02699 as candidates of TLR2-activating molecules (Fig. 1*C*). Some of the lipoproteins were identified as quinol oxidase (SAOUHSC_01002), and the ATP-binding cassette transporter (SAOUHSC_02699, SAOUHSC_00634) and the others were classified as hypothetical proteins. SAOUHSC_00634 has been previously reported as SitC, which acts as an iron-regulated ATP-binding cassette transporter in *S. aureus* and *Staphylococcus epidermidis* and is a major lipoprotein that is distributed throughout the cell wall (26). SAOUHSC_00634 and -01180 were also identified in the membrane fraction of *S. aureus* (13). Although some of lipoproteins reported (13) were not identified in our study, probably because of differences in the culture conditions, similar lipoproteins were extracted. Thus, we consider lipoproteins to be constitutively expressed in *S. aureus*.

SAOUHSC_02699, -02650, and -00634, which were separated by preparative SDS-PAGE (Fig. 2*A*), activate TLR2-expressing cells (Ba/mTLR2) but not murine TLR4- and MD-2-expressing Ba/mTLR4/mMD-2 cells or the negative control Ba/κB cells (Fig. 2*B*). They also exert strong TNF-α-inducing activity on murine and human immune cells (Fig. 2, *D* and *E*). These data indicate that the lipoproteins are the TLR2-activating ligands in *S. aureus*. Sa-M-TX contained LTA, which was visualized in the range of 15–23 kDa (Fig. 1*B*), whereas the activity of Sa-M-TX was observed in the range of 30–35 kDa (Fig. 1*B*). We have previously reported that the LTA fraction derived from an *S. aureus* lipoprotein knock-out mutant is 100-fold less potent than that of the wild-type (15). Although the LTA is still thought to be a TLR2-activating molecule (27), the principal molecules responsible for the TLR2 activity of Sa-M-TX are concluded to be lipoproteins.

Because the three lipoproteins separated were predominant constituents in Sa-M-TX and the sum of their activities is comparable with that of Sa-M-TX (Figs. 1*A* and 2*B*), they are responsible for most of the activity in Sa-M-TX. As for the TLR2-mediated recognition of whole *S. aureus*, it should include other lipoproteins, which depend on the condition of bacteria. Characterization of lipoproteins expressed in a pathogenic condition is important for the analysis of virulence factors by *S. aureus* in infectious diseases.

In the case of Gram-negative bacteria and mycoplasma, several lipoproteins have been identified as TLR2 ligands, and their N-terminal lipopeptides, which contain diacylated or triacylated *S*-(2,3-dihydroxypropyl)cystein, have been proven to be essential moieties for TLR2 activity using chemically synthesized compounds. Lipoproteins derived from Gram-negative bacteria, such as *E. coli, Borrelia burgdorferi, Neisseria gonorrhoeae,* and *Porphyromonas gingivalis,* have been proven to be triacylated lipoproteins (28–31). Mycoplasma, such as *Mycoplasma fermentans* and *Mycoplasma salivarium,* have been shown to possess diacylated lipoproteins (32, 33). However, it is not clear whether the lipoproteins in Gram-positive bacteria are diacylated or triacylated. In this study, we identified the N-terminal structure of *S. aureus* lipoprotein SAOUHSC_02699 as diacylated lipoproteins (Fig. 3). We also confirmed its activity using a synthetic counterpart (Fig. 4). In several bacteria, but not all, the N terminus of the diacylglyceryl-modified cysteine residue is fatty-acylated by a lipoprotein *N*-acyltransferase (*lnt*) (34). Stoll *et al.* (13) screened the published genome sequences of *S. aureus* strains for a gene encoding an *lnt* homolog and found no such protein. These data correspond to our data that the lipoproteins in *S. aureus* are diacylated.

Kurokawa *et al.* (35) recently reported that N terminus of *S. aureus* SitC lipoprotein is triacylated. They also suggested the existence of another type of *N*-acyltransferase distinct from *lnt*. Although the results did not agree with our analytical data, it is possible to consider that strain variation or cultural condi-

tion may affect the activity of the suggested enzyme. Further analysis must be necessary.

In conclusion, we identified TLR2-activating lipoproteins from *S. aureus* cells and characterized the N-terminal lipopeptide structure of a lipoprotein SAUOHSC_02699 as a diacylated one. Because these lipoproteins are considered to contribute to the virulence of *S. aureus*, further studies using protein expression or organic synthetic chemistry are now ongoing to clarify their immunobiological properties.

Acknowledgments—We thank Professor Kazuhisa Sugimura at Kagoshima University for measuring luciferase activity.

REFERENCES

1. Lowy, F. D. (1998) *N. Engl. J. Med.* **339,** 520–532
2. Takeuchi, O., Hoshino, K., Kawai, T., Sanjo, H., Takada, H., Ogawa, T., Takeda, K., and Akira, S. (1999) *Immunity* **11,** 443–451
3. Schwandner, R., Dziarski, R., Wesche, H., Rothe, M., and Kirschning, C. J. (1999) *J. Biol. Chem.* **274,** 17406–17409
4. Travassos, L. H., Girardin, S. E., Philpott, D. J., Blanot, D., Nahori, M. A., Werts, C., and Boneca, I. G. (2004) *EMBO Rep.* **5,** 1000–1006
5. Inohara, N., Ogura, Y., Fontalba, A., Gutierrez, O. Pons, F., Crespo, J., Fukase, K., Inamura, S., Kusumoto, S., Hashimoto, M., Foster, J. S., Moran, P. A., Fernandez-Luna, L. J., and Nuñez, G. (2003) *J. Biol. Chem.* **278,** 5509–5512
6. Chamaillard, M., Hashimoto, M., Horie, Y., Masumoto, J., Qiu, S., Saab, L., Ogura, Y., Kawasaki, A., Fukase, K., Kusumoto, S., Valvano, M. A., Foster, S. J., Mak, T. W., Nuñez, G., and Inohara, N. (2003) *Nat. Immunol.* **4,** 702–707
7. Morath, S., Geyer, A., and Hartung, T. (2001) *J. Exp. Med.* **193,** 393–397
8. Suda, Y., Tochio, H., Kawano, K., Takada, H., Yoshida, T., Kotani, S., and Kusumoto, S. (1995) *FEMS Immunol. Med. Microbiol.* **12,** 97–112
9. Hashimoto, M., Yasuoka, J., Suda, Y., Takada, H., Yoshida, T., Kotani, S., and Kusumoto, S. (1997) *J. Biochem.* **121,** 779–786
10. Han, S. H., Kim, J. H., Martin, M., Michalek, S. M., Nahm, M. H. (2003) *Infect. Immun.* **71,** 5541–5548
11. Hashimoto, M., Imamura, Y., Morichika, T., Arimoto, K., Takeuchi, O., Takeda, K., Akira, S., Aoyama, K., Tamura, T., Kotani, S., Suda, Y., and Kusumoto, S. (2000) *Biochem. Biophys. Res. Commun.* **273,** 164–169
12. Hashimoto, M., Tawaratsumida, K., Kariya, H., Aoyama, A., Tamura, T., and Suda, Y. (2006) *Int. Immunol.* **18,** 355–362
13. Stoll, H., Dengjel, J., Nerz, C., and Götz, F. (2005) *Infect. Immun.* **73,** 2411–2423
14. Bubeck, J. W., Williams, W. A., and Missiakas, D. (2006) *Proc. Natl. Acad. Sci. U. S. A.* **103,** 13831–13836
15. Hashimoto, M., Tawaratsumida, K., Kariya, H., Kiyohara, A., Suda, Y., Krikae, F., Kirikae, T., and Götz, F. (2006) *J. Immunol.* **177,** 3162–3169
16. Iordanescu, S., and Surdeanu, M. (1976) *J. Gen. Microbiol.* **96,** 277–281
17. Shibata, K., Hasebe, A., Sasaki, T., and Watanabe, T. (1997) *FEMS Immunol. Med. Microbiol.* **19,** 275–283
18. Hirschfeld, M., Ma, Y, Weis, J. H., Vogel, S. N., and Weis, J. J. (2000) *J. Immunol.* **165,** 618–622
19. Laemmli, U. K. (1970) *Nature* **227,** 680–685
20. Wallis, R. S., Amir-Tahmasseb, M., and Ellner, J. J. (1990) *Proc. Natl. Acad. Sci. U. S. A.* **87,** 3348–3352
21. Towbin, H., Staehelin, T., and Gordon, J. (1979) *Proc. Natl. Acad. Sci. U. S. A.* **76,** 4350–4354
22. Jensen, O. N., Wilm, M., Shevchenko, A., and Mann, M. (1999) *Methods Mol. Biol.* **112,** 513–530
23. Perkins, D. N., Pappin, D. J., Creasy, D. M., and Cottrell, J. S. (1999) *Electrophoresis* **20,** 3551–3567
24. Masuda, T., Tomita, M., and Ishihama, Y. (2007) *J. Proteome Res.* **7,** 731–740
25. Hantke, K., and Braun, V. (1973) *Eur. J. Biochem.* **34,** 284–296
26. Cockayne, A., Hill, J. P., Powell, N. B., Bishop, K., Sims, C., and Williams, P. (1998) *Infect. Immun.* **66,** 3767–3774
27. Schröder, N. W., Morath, S., Alexander, C., Hamann, L., Hartung, T., Zähringer, U., Göbel, B. U., Webe, R., Jr., and Schumann, R. R. (2003) *J. Biol. Chem.* **278,** 15587–15594
28. Hirschfeld, M., Kirschning, C. J., Schwandner, R., Wesche, H., Weis, J. H., Wooten, R. M., and Weis, J. J. (1999) *J. Immunol.* **163,** 2382–2386
29. Lee, H. K., Lee, J., and Tobias, S. P. (2002) *16 J. Immunol.* **8,** 4007–4012
30. Fisette, P. L., Ram, S., Andersen, M. J., Guo, W., and Ingalls, R. R. (2003) *J. Biol. Chem.* **278,** 46252–46260
31. Hashimoto, M., Asai, Y., and Ogawa, T. (2004) *Int. Immunol.* **16,** 431–437
32. Mühlradt, P. F., Kiess, M., Meyer, H., Süssmuth, R., and Jung, G. (1997) *J. Exp. Med.* **185,** 1951–1958
33. Shibata K, Hasebe, A., Into, T., Yamada, M., and Watanabe, T. (2000) *J. Immunol.* **165,** 6538–6544
34. Sankaran, K., and Wu, H. C. (1994) *J. Biol. Chem.* **269,** 19701–19706
35. Kurokawa, K., Lee, H., Roh, K-B., Asanuma, M., Kim, Y. S., Nakayama, H., Shiratsuchi, A., Choi, Y., Takeuchi, O., Kang, H. J., Dohmae, N., Nakanishi, Y., Akira, S., Sekimizu, K., and Lee, B. L. (January 12, 2009) *J. Biol. Chem.* 10.1074/jbc.M809618200